AD-A068 598 LOCKHEED MISSILES AND SPACE CO INC PALO ALTO CALIF PA--ETC F/G 20/11
A VARIABLE-STEP CENTRAL DIFFERENCE METHOD FOR STRUCTURAL DYNAMI--ETC(U)
APR 79 K C PARK, P G UNDERWOOD N00014-74-C-0355

UNCLASSIFIED LMSC/D626886 NL

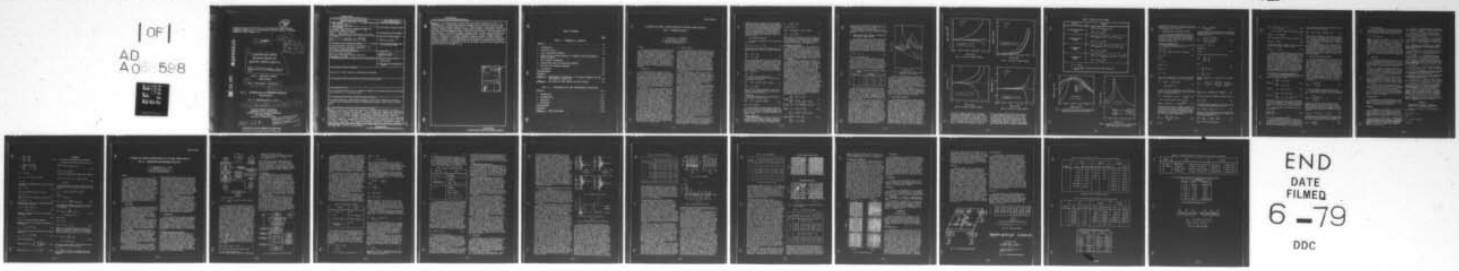

END
DATE FILMED
6-79
DDC

Research sponsored by the Office of Naval Research under Contract N00014074-C-0355 and by the Independent Research Program of Lockheed Missiles & Space Company, Inc.

(12) 35p.

(11) Apr[illegible]1979

(6)

A VARIABLE-STEP CENTRAL DIFFERENCE METHOD FOR STRUCTURAL DYNAMICS ANALYSIS.

Part I. Theoretical Aspects. Part II. Implementation and Performance Evaluation.

PART I: THEORETICAL ASPECTS

(LMSC-D626886)

(10) by K. C. Park and P. G. Underwood

(15) N00014-74-C-0355

PART II: IMPLEMENTATION AND PERFORMANCE EVALUATION

(LMSC-D633782)

by P. G. Underwood and K. C. Park

(14) LMSC/D626886, LMSC/D633782

Applied Mechanics Laboratory
Department 52-33, Building 205
Lockheed Palo Alto Research Laboratory
3251 Hanover Street
Palo Alto, California 94304

210 118

JOB

LOCKHEED PALO ALTO RESEARCH LABORATORY
LOCKHEED MISSILES & SPACE COMPANY, INC.
A SUBSIDIARY OF LOCKHEED AIRCRAFT CORPORATION

UNCLASSIFIED

SECURITY CLASSIFICATION OF THIS PAGE (When Data Entered)

REPORT DOCUMENTATION PAGE		READ INSTRUCTIONS BEFORE COMPLETING FORM
1. REPORT NUMBER LMSC-D626686 (Part I) LMSC-D633782 (Part II)	2. GOVT ACCESSION NO.	3. RECIPIENT'S CATALOG NUMBER
4. TITLE (and Subtitle) A VARIABLE-STEP CENTRAL DIFFERENCE METHOD FOR STRUCTURAL DYNAMICS ANALYSIS PART I: Theoretical Aspects PART II: Implementation & Performance Evaluation		5. TYPE OF REPORT & PERIOD COVERED 6. PERFORMING ORG. REPORT NUMBER
7. AUTHOR(s) Part I: K. C. Park and P. G. Underwood Part II: P. G. Underwood and K. C. Park		8. CONTRACT OR GRANT NUMBER(s) N00014-74-C-0355
9. PERFORMING ORGANIZATION NAME AND ADDRESS Applied Mechanics Laboratory (52-33/205) Lockheed Palo Alto Research Laboratory Palo Alto, California 94304		10. PROGRAM ELEMENT, PROJECT, TASK AREA & WORK UNIT NUMBERS
11. CONTROLLING OFFICE NAME AND ADDRESS Office of Naval Research Structural Mechanics Program (Code 474) Arlington, VA 22217		12. REPORT DATE April 17, 1979 13. NUMBER OF PAGES 22
14. MONITORING AGENCY NAME & ADDRESS(if different from Controlling Office)		15. SECURITY CLASS. (of this report) Unclassified 15a. DECLASSIFICATION/DOWNGRADING SCHEDULE

16. DISTRIBUTION STATEMENT (of this Report)

Approved for public release; distribution unlimited.

17. DISTRIBUTION STATEMENT (of the abstract entered in Block 20, if different from Report)

18. SUPPLEMENTARY NOTES

To be presented at the 3rd U. S. National Congress on Pressure Vessels and Piping, San Francisco, CA, 25-29 June 1979.

19. KEY WORDS (Continue on reverse side if necessary and identify by block number)

Structural dynamics, computational methods, direct time integration technique, variable-step integration, explicit integration formulas, error control strategies.

20. ABSTRACT (Continue on reverse side if necessary and identify by block number)

Part I: Three major theoretical aspects of variable-step explicit integration procedures are proposed and analyzed. These include basic fixed-step integration formulas for no damping, diagonal damping and nondiagonal damping problems; the adjustment of the basic formulas to accommodate step changes; and, step size selection criteria. It is shown that the truncation error concept is not adequate to detect numerical instability for general structural dynamics analysis when low accuracy is requested. The "apparent frequency" concept is introduced to maximize stable step sizes and is shown to be stable when low accuracy is requested.

DD FORM 1 JAN 73 1473 EDITION OF 1 NOV 65 IS OBSOLETE

UNCLASSIFIED

SECURITY CLASSIFICATION OF THIS PAGE (When Data Entered)

PART II: The variable-step central difference method developed in Part I is implemented as a stand-alone software package that is easily accessed by existing structural dynamics analyzers (i.e., finite-element, -difference discrete element computer codes) through a common data structure, input/output (I/O) manager and a few user-supplied control and interface routines. The performance of this package is evaluated through a computer study of four sample problems that embody a large class of response characteristics: linear to highly nonlinear; wave to structural to uncoupled component response; narrow to wide frequency spread; no damping to over-damping and accuracy-critical to numerical-stability-critical response. The present method is successful in meeting these response characteristics with effectiveness in all the above cases with the single exception of pure wave propagation.

TABLE OF CONTENTS

A VARIABLE-STEP CENTRAL DIFFERENCE METHOD FOR STRUCTURAL DYNAMICS ANALYSIS

PART I: THEORETICAL ASPECTS

K. C. PARK AND P. G. UNDERWOOD
Applied Mechanics Laboratory
Lockheed Palo Alto Research Laboratory
Palo Alto, California 94304

ABSTRACT

Three major theoretical aspects of variable-step explicit integration procedures are proposed and analyzed. These include basic fixed-step integration formulas for no damping, diagonal damping and nondiagonal damping problems; the adjustment of the basic formulas to accommodate step changes; and, step size selection criteria. It is shown that the truncation error concept is not adequate to detect numerical instability for general structural dynamics analysis when low accuracy is requested. The "apparent frequency" concept is introduced to maximize stable step sizes and is shown to be stable when low accuracy is requested.

1. INTRODUCTION

The central difference integration formula is widely used for direct time integration of the equations of motion governing structures. This popularity is due to its favorable fixed-step stability limit for undamped problems, no numerical damping, low frequency distortion, and simple implementation. The formula is thus well suited for fixed-step integration cases provided the step size chosen does not exceed its stability limit with respect to the highest frequency of the system under consideration and the solution accuracy is not adversely affected by such a step size choice.

In practice, however, step size changes are often desired to select a step size as large as possible, consistent with a specified local error. This calls for an adaptation of the central difference formula to a variable-step integration procedure. There are four major factors that affect the efficiency of a variable-step integration procedure: the basic integration formula which dictates stability and accuracy for fixed-step integration; the adjustment of the basic formula to handle step size changes and to minimize any loss of stability and accuracy; the step size selection strategy to satisfy a specified error bound and at the same time to avoid instability; and and last, but not least, the computer implementation.

This paper is divided into two parts to address the above four factors. In Part I we concentrate on the first three factors as they are closely tied to the algorithmic nature of the integration process. Thus, Part I covers theoretical aspects of the variable-step integration package. Part II (1) describes the computer implementation and the performance evaluation of the package through carefully chosen numerical experiments. The many "ifs" to treat the many "exceptions" that accompany a typical software development process are also presented.

2. OUTLINE OF PART I

The stability and accuracy characteristics of the fixed-step central difference formula are well understood for undamped equations of motion governing structures, cf., Kreig and Key (2) or Park (3). The effect of system damping on its performance, however, is not well understood even though it is generally acknowledged that the presence of nondiagonal damping reduces its stability margin. In Section 3 the basic formulas for the fixed-step integration are presented for undamped, diagonally damped and nondiagonally damped cases. In Section 4 the analysis of stability and accuracy of the formulas for the nondiagonally damped equations of motion is presented. The origin of the stability reduction due to nondiagonal damping is identified and a means to minimize this stability reduction is given.

The step adjustment techniques are described in Section 5. Two techniques are introduced to adjust the basic integration formula to accommodate step size changes: interpolation of past solutions to represent solution vectors at equal intervals of the present step size and adoption of variable coefficients in the integration formula. Care is taken so that either technique retains the characteristics, as close as possible, of the fixed-step formula.

The heart of the present paper is concerned with step size selection strategies. Several variable-step integration procedures have been proposed for explicit methods, notably, by Krogh (4), Brayton et al. (5), Gordon and Shampine (6), Zadunaisky (7), among others. While the details of these procedures vary considerably, their common presumption is that the local truncation error is a reliable measure to control step size changes. Although this appears to be the case for high-accuracy requirements, i.e., the relative local error is less than 10^{-5}, its applicability to oscillatory problems such as structural dynamics problems has not been firmly established. Moreover, in typical structural dynamics analysis much lower accuracy (say, a few percent relative error) is often satisfactory due to analysis cost and uncertainties in structural modeling. In Section 6, the applicable ranges of truncation error-based step selection criteria are examined. This examination indicates that for low-accuracy analysis the truncation error concept is unreliable. The step size is either too conservative so that it yields more accuracy than requested or too unconservative; hence, the step size is seldom the one desired.

In Section 7 we present a new step size selection criterion. The criterion is based on the sampling concept of oscillating signals, in which frequencies are determined from the "apparent" oscillations of the solution components. Here we have been guided by

heuristic schemes as the theory is still incomplete. Nevertheless, the key feature of the new criterion is shown to have a sound foundation from the viewpoint of the Courant-Fisher maximum-minimum theorem of eigenvalues (9). The numerical experiments presented in Part II illustrate that the new step size selection criterion exhibits fidelity to a prescribed error bound and safeguards against numerical instability. A summary of the new results presented in Part I is given in Section 8.

3. BASIC INTEGRATION FORMULAS

For direct time integration of the discrete equations of motion

$$\underset{\sim}{M}\,\ddot{\underline{u}}^n + \underset{\sim}{D}\,\dot{\underline{u}}^n + \underline{f}\,(\underline{u}^n) = \underline{P}\,(t^n) \tag{1}$$

governing structural dynamics, the summed form of the central difference formula for fixed-step integration is

$$\begin{aligned} \dot{\underline{u}}^{n+\frac{1}{2}} &= \dot{\underline{u}}^{n-\frac{1}{2}} + h\,\ddot{\underline{u}}^n \\ \underline{u}^{n+1} &= \underline{u}^n + h\,\dot{\underline{u}}^{n+\frac{1}{2}} \end{aligned} \tag{2}$$

where $\underline{u}$ is the displacement vector, h the fixed-step size, the superscript $(\_)^n$ indicates the vector value at the discrete time t^n, the superscript dot ($\dot{}$) temporal differentiation, $\underset{\sim}{M}$ and $\underset{\sim}{D}$ are the diagonal mass and damping matrices, $\underline{f}\,(\underline{u})$ is the set of internal forces due to stiffness that oppose the structural motion (stiffness forces), and $\underline{P}\,(t^n)$ is the applied load at time t^n. For a linear problem the stiffness force $\underline{f}\,(\underline{u})$ becomes

$$\underline{f}\,(\underline{u}) = \underset{\sim}{K}\,\underline{u} \tag{3}$$

where $\underset{\sim}{K}$ is the linear stiffness matrix.

A general recursion formula is obtained by combining equations (1) and (2)

$$\begin{aligned} \dot{\underline{u}}^{n+\frac{1}{2}} &= \dot{\underline{u}}^{n-\frac{1}{2}} + h\,\underset{\sim}{M}^{-1}\,[\underline{P}^n - \underset{\sim}{D}\,\dot{\underline{u}}^n - \underline{f}\,(\underline{u}^n)] \\ \underline{u}^{n+1} &= \underline{u}^n + h\,\dot{\underline{u}}^{n+\frac{1}{2}} \end{aligned} \tag{4}$$

Equation (4) will now be specialized to three basic formulas to treat undamped, diagonally damped, and nondiagonally damped problems.

Undamped Case

This case corresponds to $\underset{\sim}{D} = \underset{\sim}{0}$ in equation (4) and the recursion formula becomes

$$\begin{aligned} \dot{\underline{u}}^{n+\frac{1}{2}} &= \dot{\underline{u}}^{n-\frac{1}{2}} + h\,\underset{\sim}{M}^{-1}\,[\underline{P}^n - \underline{f}\,(\underline{u}^n)] \\ \underline{u}^{n+1} &= \underline{u}^n + h\,\dot{\underline{u}}^{n+\frac{1}{2}} \end{aligned} \tag{5}$$

It is well known that the above recursion formula enjoys the full accuracy of the integration formula (2) and there is no reduction of the stability margin from $\omega_{max}\,h \le 2$, where ω_{max} is the highest frequency of the undamped system.

Diagonally Damped Case

When damping is present, difficulty arises in the computation of $\underset{\sim}{D}\,\dot{\underline{u}}^n$ because the velocity vectors are computed at half-step points. The best known answer to this difficulty is to linearly interpolate $\dot{\underline{u}}^n$ as

$$\dot{\underline{u}}^n = \frac{1}{2}\,(\dot{\underline{u}}^{n+\frac{1}{2}} + \dot{\underline{u}}^{n-\frac{1}{2}}) \tag{6}$$

to obtain from (4)

$$\begin{aligned} \dot{\underline{u}}^{n+\frac{1}{2}} &= \underset{\sim}{E}_1^{-1}\left(\underset{\sim}{E}_2\,\dot{\underline{u}}^{n-\frac{1}{2}} + h\,[\underline{P}^n - \underline{f}\,(\underline{u}^n)]\right) \\ \underline{u}^{n+1} &= \underline{u}^n + h\,\dot{\underline{u}}^{n+\frac{1}{2}} \end{aligned} \tag{7}$$

where $\underset{\sim}{E}_1 = \underset{\sim}{M} + \frac{1}{2}\,h\,\underset{\sim}{D}$ and $\underset{\sim}{E}_2 = \underset{\sim}{M} - \frac{1}{2}\,h\,\underset{\sim}{D}$. Notice that the inversion of the matrix E_1 presents no computational difficulty as it involves only a combination of two diagonal matrices. The stability limit of (7) is known to be the same as the undamped case (3).

Nondiagonally Damped Case

In this case formula (7) is not applicable as it loses the simplicity of vector operations due to the attendant nondiagonal factoring of $\underset{\sim}{E}_1$. In order to preserve the vector calculation advantage of the explicit formula (2), the term $\underset{\sim}{D}\,\dot{\underline{u}}^n$ needs to be approximated. The effects of approximating $\underset{\sim}{D}\,\dot{\underline{u}}^n$ on numerical stability has been evaluated in (3). The results show that as the damping increases the stability limit of the central difference formula is reduced for all cases examined.

The possibility of minimizing the reduction of the nondiagonal damping-induced stability margin was initially studied in (9). The underlying observation to be exploited for this minimization is that the stiffness force and the damping terms can be separated, and the accuracy of the stiffness force term is not affected by the choices for approximating $\dot{\underline{u}}^n$. This suggests iterations on the damping term as a profitable avenue if the gain from minimizing the stability reduction outweighs the overhead for iterating the damping term. This is in general the case for nonlinear problems as the evaluation of the stiffness force term constitutes the bulk of the computational effort and the damping term often remains linear.

In principle, iterations on the damping term $\underset{\sim}{D}\,\dot{\underline{u}}^n$ will improve both accuracy and stability. In practice, however, the number of iterations on $\underset{\sim}{D}\,\dot{\underline{u}}^n$ has to be limited because the increase in the stability margin and accuracy from additional iterations has been shown to diminish beyond the first two iterations (9) and there is the possibility of rejecting the solution at that very time step even if the damping computation has converged. Therefore, we limit the iterations on the damping term to two at most and the resulting basic formula takes the form of

$$\text{Predict:}\quad \begin{cases} \dot{\underline{u}}_p^n = \dot{\underline{u}}^{n-\frac{1}{2}} + \gamma\,h\,\ddot{\underline{u}}^{n-1} \\ \ddot{\underline{u}}_p^n = \underset{\sim}{M}^{-1}\,[\underline{P}^n - \underset{\sim}{D}\,\dot{\underline{u}}_p^n - \underline{f}\,(\underline{u}^n)] \end{cases} \tag{8}$$

$$\text{Correct:}\quad \dot{\underline{u}}_c^n = \dot{\underline{u}}^{n-\frac{1}{2}} + \frac{h}{2}\,[\beta\,\ddot{\underline{u}}_p^n - (1-\beta)\,\ddot{\underline{u}}^{n-1}] \tag{9}$$

$$\text{Modify:}\quad \dot{\underline{u}}^n = \alpha\,\dot{\underline{u}}_c^n + (1-\alpha)\,\dot{\underline{u}}_p^n \tag{10}$$

$$\text{Advance:}\quad \begin{cases} \ddot{\underline{u}}^n = \underset{\sim}{M}^{-1}\,[\underline{P}^n - \underline{f}\,(\underline{u}^n) - \underset{\sim}{D}\,\dot{\underline{u}}^n] \\ \dot{\underline{u}}^{n+\frac{1}{2}} = \dot{\underline{u}}^{n-\frac{1}{2}} + h\,\ddot{\underline{u}}^n \\ \underline{u}^{n+1} = \underline{u}^n + h\,\dot{\underline{u}}^{n+\frac{1}{2}} \end{cases} \tag{11}$$

where γ and β are integration parameters and α is an averaging parameter selected to minimize the loss of the stability margin, see Stetter (10).

We now examine the stability and the accuracy of formulas (8) through (11) for the nondiagonally damped problem.

4. STABILITY AND ACCURACY ANALYSIS OF FORMULAS FOR NON-DIAGONALLY DAMPED PROBLEMS

The analysis procedure for stability and accuracy of integration formulas for linear (or linearized) equations of motion is well known, e.g., Gear (11) and Hall and Watt (12). For structural dynamic equations the reader is referred to Nickell (13), Krieg and Key (2), Bathe and Wilson (14), and Park (15), among others. For the linear case, it is well known that the integration procedure can be characterized by considering the homogeneous modal form of equation (1) as

$$\ddot{u} + 2\xi\omega\dot{u} + \omega^2 u = 0 \qquad (12)$$

where ξ is the damping ratio.

The task of determining suitable sets of parameters α, β and γ in equations (8) to (10) was presented to the computer (see Appendix A for details); where the values $\alpha = (0.0 \sim 1.0)$, $\beta = (0.0 \sim 1.0)$ and $\gamma = (0.0 \sim 0.5)$ were considered. Of all combinations of these parameter ranges, four sets of parameters, summarized in Table 1, were chosen for actual implementation due to their favorable stability margins.

Table 1 Candidate formulas for nondiagonally damped problems

Formula	Parameters
F1	$\alpha = 0.5$, $\beta = 1.0$, $\gamma = 0$
F2	$\alpha = 0.5$ $\beta = 1.0$, $\gamma = 0.5$
F3	$\alpha = 0.75$, $\beta = 0.75$, $\gamma = 0.5$
F4	$\alpha = 1.0$, $\beta = 1.0$, $\gamma = 0.0$
F5	$\alpha = 0.0$, $\beta = 1.0$, $\gamma = 0.0$

Figure 1 shows the stability limits of the four formulas, along with the conventional formula (F5), in terms of the normalized step size ωh vs. the damping ratio ξ. Observe from Figure 1 that the choice of parameters α, β and γ has a dramatic effect on the stability limit. For example, it suggests a smaller value of α in equation (10) if the damping ratio (ξ) associated with the highest frequency is greater than 0.5 and vice versa.

Figure 2 shows the accuracy characteristics of formulas (F1) and (F4) in Table 1 and of formula (7) for the diagonally damped case (see Appendix A for accuracy definitions). Notice that when the system is lightly damped, i.e., $\xi \leq 0.1$, formula (F4) is more accurate than formula (F1). This is because within the neighborhood of $\xi \leq 0.1$, formula (F4) enjoys a larger stability margin than formula (F1), as can be observed from Figure 1. Formulas (F2) and (F3) have more or less similar accuracy characteristics as formula (F1) as their stability characteristics are quite similar. The accuracy characteristics of Formula (F5) are not included as it is the least desirable from a stability viewpoint (see Figure 1). It is emphasized, however, that formula (F5) has been used in many existing explicit integration packages to treat nondiagonal damping in the equations of motion.

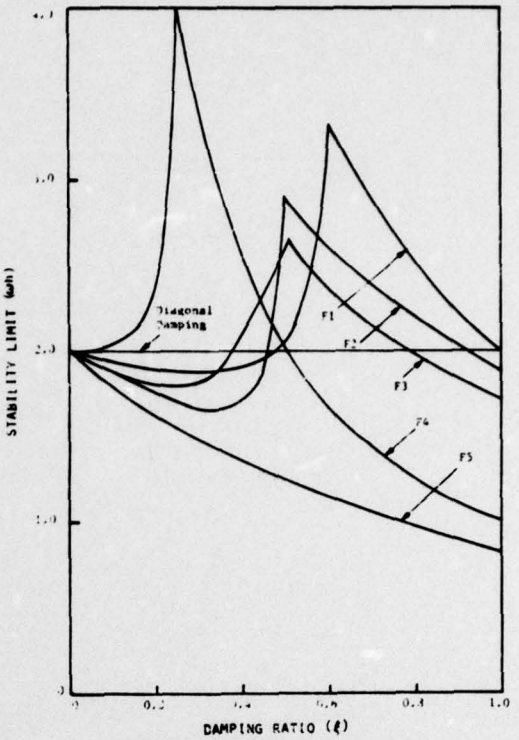

Fig. 1 Stability limits of basic formulas (see Table 1 for formulas)

From the foregoing analysis of stability and accuracy of the four basic formulas we have chosen formula (F1) for heavily damped problems, formula (F4) for lightly damped problems, and formula (7) for diagonally damped problems. In practice, however, an accurate estimate of the damping coefficient associated with the highest frequency of the system is often difficult or even impossible. Under such situations, formula (F1) is adopted as a default.

So far in this section, fixed-step formulas for various system characterizations have been discussed. When the step size changes, one must accommodate the effect of the step size change on each basic formula. This will be dealt with in the next section.

5. STEP CHANGING TECHNIQUES

It was pointed out in Section 2 that step size changes can be accommodated either by interpolation of past solutions or the use of variable coefficients in the integration formula. In general, interpolation requires additional solution vectors to be stored in order to obtain solution vectors at equal step intervals of the present step size. The introduction of variable coefficients alleviates this additional storage requirement, but is known to cause instability if the step size is changed too often (16). In this study, four step changing techniques have been developed and they are summarized in Table 2. Note that step size changes affect the stability only at one step, viz., the time step at which the step size is changed. This is because the formula for computing the displacement vector is the same for all step changing techniques. Thus, in order to examine the effect of step size changes on the local stability of

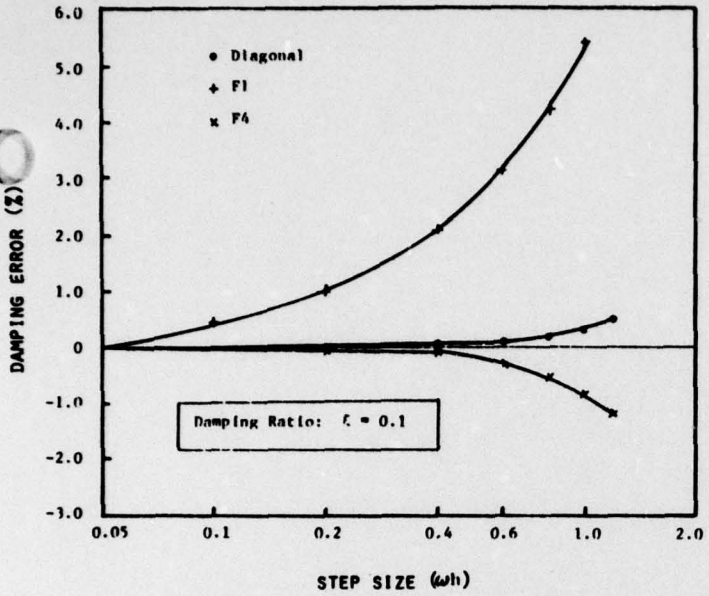

Fig. 2a Accuracy of basic formulas

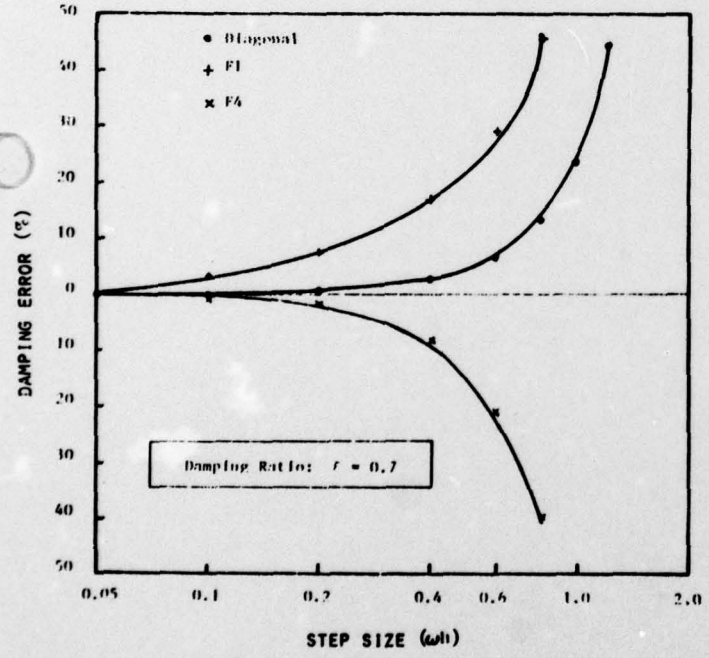

Fig. 2b Accuracy of basic formulas

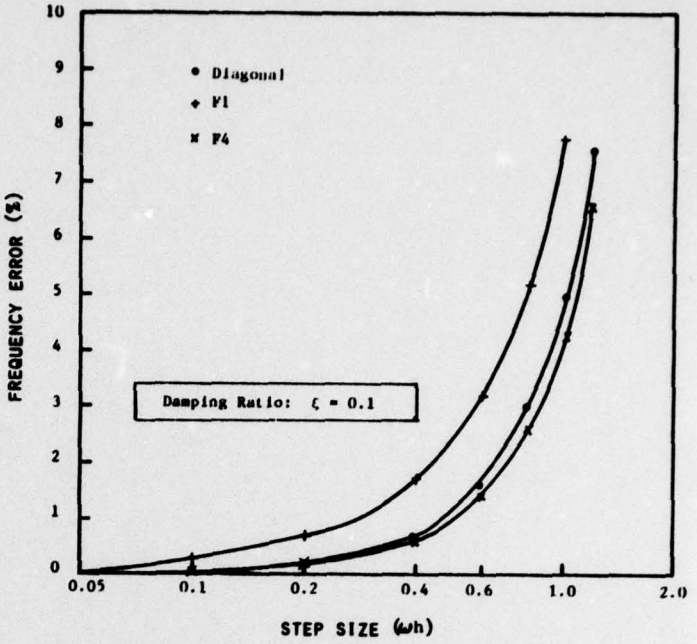

Fig. 2c Accuracy of basic formulas

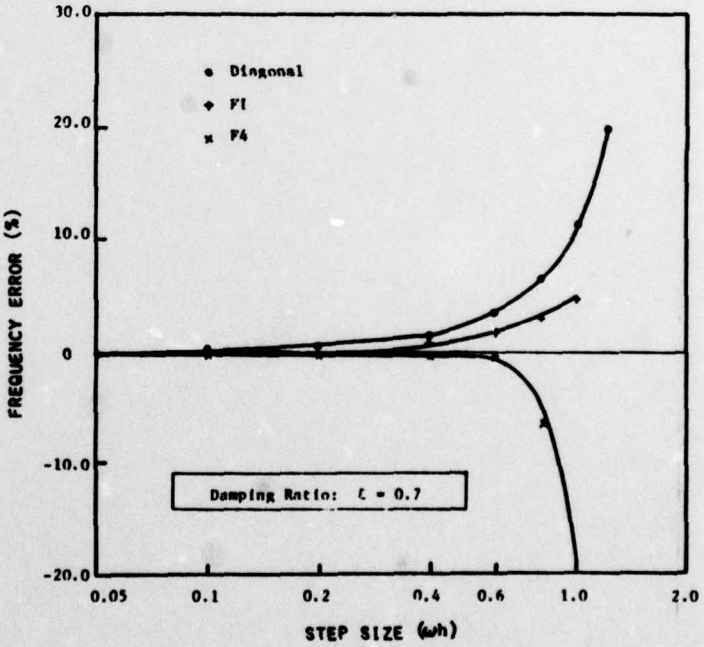

Fig. 2d Accuracy of basic formulas

this type of integration procedure, it suffices to examine how the amplification factor λ will behave when the step size is changed. The reader is referred to Appendix B for details of the derivation of the local stability polynomials, and the results are summarized in Figures 3 and 4 for the values of $\alpha \cdot \beta = 0.5$ and $\gamma = 0$ in equations (8) through (11). Notice from Figure 3 that, when increasing the step size, the velocity averaging technique (FAVE) is most desirable for undamped problems, whereas the variable coefficient method (FVCO) outperforms the rest for heavily damped problems. When reducing the step size, both the extrapolation (FEXT) and the interpolation (FINT) techniques become identical and superior to the FVCO for lightly damped problems. However, the egg-shaped unstable zones in Figure 4 for heavily damped problems

Table 2 Formulas for step changes

Technique	Formula
Variable Coefficient (FVCO)	$\dot{u}^{n+\frac{1}{2}} = \dot{u}^{n-\frac{1}{2}} + \frac{1}{2}(h_n+h_{n-1})\ \ddot{u}^n$ $u^{n+1} = u^n + h_n\ \dot{u}^{n+\frac{1}{2}}$
Average Velocity (FAVE)	$\dot{u}^{n+\frac{1}{2}} = \frac{1}{2}[(3-r)\ \dot{u}^{n-\frac{1}{2}} - (1-r)\ \dot{u}^{n-\frac{3}{2}}] + h_n\ddot{u}^n$ $u^{n+1} = u^n + h_n\ \dot{u}^{n+\frac{1}{2}}$
Extrapolation (FEXT)	$\dot{u}^{n+\frac{1}{2}} = \frac{1}{8}[(7+r^2)\ \dot{u}^{n-\frac{1}{2}} - (1-r^2)\ \dot{u}^{n-\frac{3}{2}}] + h_n\ddot{u}^n$ $u^{n+1} = u^n + h_n\ \dot{u}^{n+\frac{1}{2}}$
Interpolation (FINT)	$\dot{u}^{n+\frac{1}{2}} = \dot{u}^{n-\frac{1}{2}} + \frac{1}{8}(h_n+h_{n-1})\ [(3+r)\ddot{u}^n + (1-r)\ddot{u}^{n-1}]$ $u^{n+1} = u^n + h_n\ \dot{u}^{n+\frac{1}{2}}$
1) $r = h_n/h_{n-1}$ 2) All the above formulas recover the basic formula (2) when $r = 1$.	

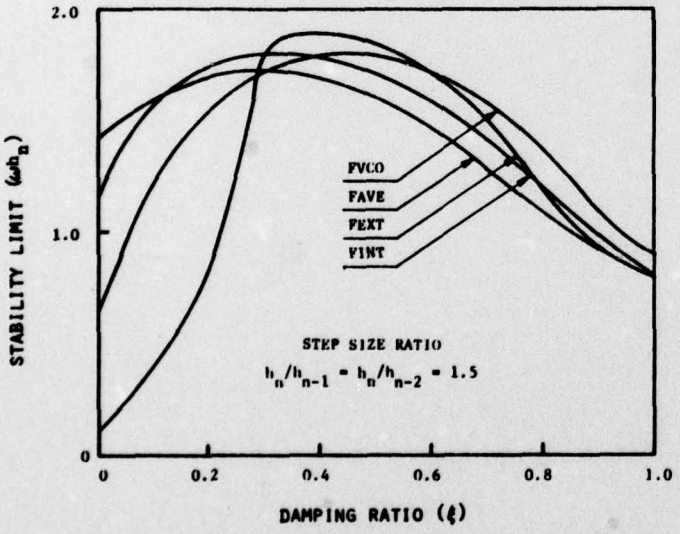

Fig. 3 Local stability of various step increasing techniques (see Table 2 for formulas)

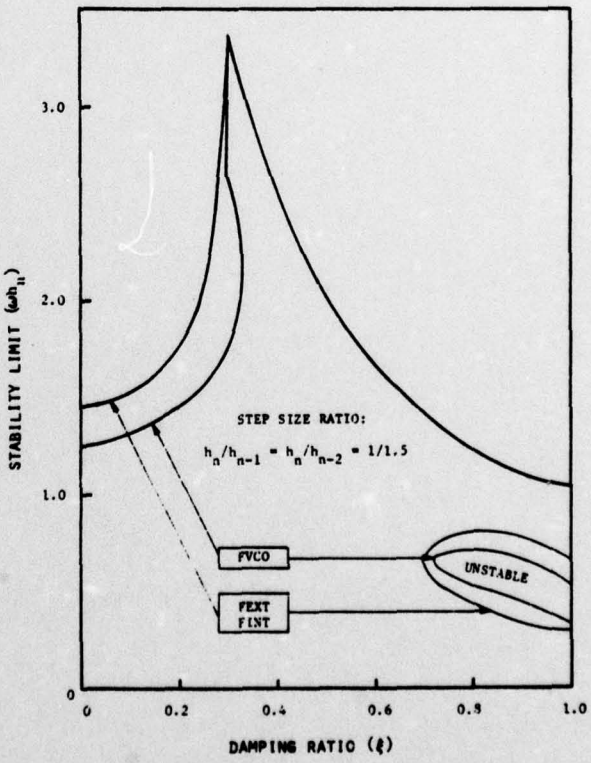

Fig. 4 Stability of various step reducing techniques (see Table 2 for formulas)

suggest that one should use the FVCO due to its smaller unstable zone. This will be further elaborated in the Evaluation section of Part II.

6. CONVENTIONAL STEP SIZE SELECTION STRATEGY

In this section, two conventional step size selection criteria will be analyzed: the truncation error and the difference in the predictor-corrector solutions. It will be shown that, when low accuracy is requested, these criteria are either unreliable and/or too expensive to use.

Analysis of Truncation Error

In order to make our point clear, we will use the linear homogeneous undamped problem, viz.,

$$\underset{\sim}{M}\,\ddot{\underline{u}}^n + \underset{\sim}{K}\,\underline{u}^n = 0 \tag{13}$$

which can be decomposed into modal components

$$\ddot{\underline{q}}^n + \underset{\sim}{\Lambda}\,\underline{q}^n = 0 \tag{14}$$

where

$$\underline{u} = \underset{\sim}{T}\,\underline{q}$$

$$\underset{\sim}{T}^t\,\underset{\sim}{M}\,\underset{\sim}{T} = \underset{\sim}{I}$$

$$\underset{\sim}{T}^T\,\underset{\sim}{K}\,\underset{\sim}{T} = \underset{\sim}{\Lambda}$$

$$\underset{\sim}{\Lambda} = [\omega_i^2]$$

The local truncation error of the central difference method (2) for integrating (13) can be expressed as

$$\underline{\tau}^{n+1} = \frac{h^3}{12}\dddot{\underline{u}}^n = -\frac{h^3}{12}\underset{\sim}{M}^{-1}\underset{\sim}{K}\,\ddot{\underline{u}}^n \simeq -\frac{h^2}{12}\underset{\sim}{M}^{-1}\underset{\sim}{K}(\underline{u}^{n+1} - \underline{u}^n) \tag{15}$$

A proper local error measurement for the explicit formula is to evaluate component-wise relative errors and take the maximum among them, viz.,

$$\varepsilon^{n+1} = \max\left\{|\tau_1/u_1|,\ |\tau_2/u_2|,\ \ldots\ |\tau_N/u_N|\right\} \tag{16}$$

It must be noted that error norms of ℓ_p-type

$$\|\underline{\tau}/\underline{u}\|_p = \left\{|\tau_1/u_1|^p + \ldots + |\tau_N/u_N|^p\right\}^{1/p} \tag{17}$$

although they are suitable for implicit formulas, are not applicable to explicit formulas because they tend to mask out locally unstable components which propagate violently in the explicit integration process. To simplify the subsequent analysis let us introduce the k-th relative error component ε_k^{n+1} as

$$\varepsilon_k^{n+1} = -\frac{(\ddot{u}_K^{n+1} - \ddot{u}_k^n)}{u_k^{n+1}};\quad u_k^{n+1} \neq 0 \tag{18}$$

so that

$$\varepsilon^{n+1} = \frac{h^2}{12}\max_{1\le k\le N}\left\{|\varepsilon_k^{n+1}|\right\} \tag{19}$$

Upon multiplying both the numerator and the denominator by u_k^{n+1}, equation (18) can be written in terms of modal components from (14) as

$$\varepsilon_k^{n+1} = \frac{\sum_{j=1}^{N}\omega_j^2\,t_{k_j}^2\,q_j^{n+1}\,\Delta q_j^{n+1}}{\sum_{j=1}^{N}(t_{k_j}\,q_j^{n+1})^2} \tag{20}$$

where $\Delta q^{n+1} = q^{n+1} - q^n$.

Assuming that

$$\|\Delta\underline{q}/\underline{q}\|_2 \ll 1 \tag{21}$$

equation (20) can be approximated in the form

$$\varepsilon_K^{n+1} \simeq \frac{b_K^{n+1}}{a_k^{n+1}} - \frac{b_k^n}{a_k^n}$$

where

$$b_k = \sum_{j=1}^{N}\omega_j^2\,(t_{k_j}\,q_j)^2 \tag{22}$$

$$a_k = \sum_{j=1}^{N}(t_{k_j}\,q_j)^2$$

Remark: Assumption (21) is equivalent to the approximation

$$\varepsilon_k^{n+1} = -\frac{(\ddot{u}_K^{n+1} - \ddot{u}_k^n)}{u_K^{n+1}} \simeq -\left[\frac{u_k^{n+1}\,\ddot{u}_k^{n+1}}{(u_k^{n+1})^2} - \frac{u_k^n\,\ddot{u}_k^n}{(u_k^n)^2}\right] \tag{23}$$

or

$$\left\|\left\{\underline{t}_K^2\,(\underline{q} + \Delta\underline{q})\ \ \Delta\underline{q}\right\} / \left\{\underline{t}_K^2\,(\underline{q} + \Delta\underline{q})\ \underline{q}\right\}\right\|_2 \ll 1 \tag{24}$$

We now define the k-th "apparent frequency" $(\omega_A^2)_k$ as

$$(\omega_a^2)_k \triangleq \frac{b_k}{a_k} \tag{25}$$

for the k-th solution component. Then it follows from the Courant-Fischer Minimax Theorem (9) that

$$\omega_{min} \le (\Delta\omega_A^2)_k \le \omega_{max}^2,\quad k = 1, \ldots, N \tag{26}$$

Equation (22) can be interpreted as the change of the apparent frequency $(\omega_A^2)_k$ from time t^n to t^{n+1} for the k-th solution component, viz.,

$$\varepsilon_k^{n+1} = (\Delta\omega_A^2)_k = (\omega_A^2)_k^{n-1} - (\omega_A^2)_k^n \tag{27}$$

so that (19) can be expressed as

$$\varepsilon^{n+1} = \frac{h^2}{12} \left|(\Delta\omega_A^2)_k\right|_{max}, \quad k = 1, \ldots, N \tag{28}$$

For a fixed error bound ε, equation (28) allows

$$(h)^2_{max} \leq 12\ \varepsilon/(\Delta\omega_A^2)_{max} \tag{29}$$

while the maximum step size $(h_s)_{max}$ for stability is

$$(h_s^2)_{max} \leq 4/\omega^2_{max} \tag{30}$$

For stability $(h^2)_{max} \leq (h_s^2)_{max}$; hence, the step size selected based equation (29) must satisfy

$$(\Delta\omega_A^2)_{max} \geq 3\ \varepsilon\ \omega^2_{max} \tag{31}$$

Note that the apparent frequency ω_k for the solution component u_k as defined by equation (25) can be viewed as a "component-wise" Rayleigh quotient. This quotient often typifies the dominant response frequency for u_k (not necessarily the fundamental one). Furthermore, the "component-wise" Rayleigh quotients, in practice, do not change drastically from one step to the next. Consequently, $(\Delta\omega_A^2)_{max}$ will remain small. From (31) observe that as ω^2_{max} increases, one must choose a smaller error bound for stable integration. Therefore, the step size criteria based on the truncation error concept for general-purpose structural dynamics analysis is reliable only when high accuracy [small ε in (29)] is requested.

Error Analysis of a Predictor-Corrector Pair

The central difference method and the trapezoidal rule will be used as a predictor-corrector pair. A widely used starting procedure is

$$\text{Predictor:} \quad \begin{cases} \underline{\dot{u}}_p^{\frac{1}{2}} = \underline{\dot{u}}^o + \frac{1}{2}h\ \underline{\ddot{u}}^o \\ \underline{u}_p^1 = \underline{u}^o + h\ \underline{u}_p^{\frac{1}{2}} \end{cases} \tag{32}$$

$$\text{Evaluate:} \quad \underline{\ddot{u}}^1 = \underset{\sim}{M}^{-1}(\underline{f} - \underset{\sim}{K}\,\underline{u}^1) \tag{33}$$

$$\text{Corrector:} \quad \begin{cases} \underline{\dot{u}}_c^1 = \underline{\dot{u}}^o + \frac{h}{2}(\underline{\ddot{u}}^o + \underline{\ddot{u}}^1) \\ \underline{u}_c^1 = \underline{u}^o + h\,\underline{\dot{u}}^o + \frac{h}{4}(\underline{\ddot{u}}^o + \underline{\ddot{u}}^1) \end{cases} \tag{34}$$

The solution process takes the pattern of prediction (P) once and evaluation (E) and correction (C) until the solution converges, i.e., $P(EC)^k$ for k-time iterations. For subsequent steps, (32a) is replaced by (2a).

To test convergence of the $P(EC)^k$ process one usually employs

$$\left|\frac{\underline{u}_{k+1} - \underline{u}_k}{\underline{u}_{k+1}}\right|_2 \leq C \tag{35}$$

where C is a convergence threshold.

Here the convergence test (35) is used for adjusting step sizes. Notice that the central difference method as a predictor provides the required full accuracy, and the trapezoidal rule as a corrector is used merely to check stability. It can be shown from (32) - (34) that the difference $\underline{d}^{n+1}$ between the predicted and converged solution is

$$\underline{d}^{n+1} = \underline{u}_C^{n+1} - \underline{u}_P^{n+1} = \frac{h^2}{4}(\underline{\ddot{u}}^{n+1} - \underline{\ddot{u}}^n) \tag{36}$$

Note that this difference is three times the truncation error (15). Therefore, except for its increased error constant 1/4 as compared to 1/12 in equation (15), the analysis and conclusion in the previous subsection on "Analysis of Truncation Error" is applicable to equation (36).

The foregoing analysis of the truncation error-based step selection strategy and the predictor-corrector iteration procedure present structural dynamics analysts with a real dilemma in that the former is unreliable and the latter is expensive to use. This has motivated the authors to develop a new step selection strategy, described in the next section, to resolve this dilemma.

7. NEW STEP SIZE SELECTION STRATEGY

It has been demonstrated in the previous section that the use of the conventional step size selection criteria based on the truncation error concept is limited to nonstiff problems or to a high-accuracy integration requirement (cf., more than five-digit accuracy). An effective use of explicit methods, thus calls for the determination of the highest frequency of the system in order to limit the maximum step size. For nonlinear problems, however, this often presents a challenge as the highest frequency can change significantly. In addition, not all natural frequencies are excited under a given load. Therefore, one wishes to compute the highest apparent (excited) frequency in order to maximize the stable step size. To this end, a "perturbed apparent frequency" ω_{PA} is introduced in the form

$$(\omega^2_{PA})_i = \frac{\Delta u_i^{n+1} \cdot \Delta \ddot{u}_i^{n+1}}{\Delta u_i^2} \tag{37}$$

for the i-th component of the solution vector $\underline{u}$.

For the linear, homogeneous undamped problem (13), the perturbed apparent frequency (37) can be expressed as

$$(\omega^2_{PA}) \triangleq \frac{\Sigma \omega_j^2\, t_{ij}^2\, \Delta q_j^2}{\Sigma t_{ij}^2\, \Delta q_j^2}, \quad |i-j| < m_b \tag{38}$$

where (14) is used as in the derivation of (20). Comparing (38) to (25), observe that the perturbed apparent frequency $(\omega_{PA})_i$ can be viewed as the frequency associated with the i-th component-wise noise. The "maximum perturbed apparent frequency" is now defined as

$$(\omega_{PA})_{max} = \max\{(\omega_{PA})_1, \ldots, (\omega_{PA})_N\}, \tag{39}$$

Therefore, $(\omega_{PA})_{max}$ is recognized as the highest component-wise noise frequency that is noticeable (apparent); hence $(\omega_{PA})_{max}$ can be used to determine h_{max},

$$h_{max} \leq \frac{2}{(\omega_{PA})_{max}}, \tag{40}$$

for stable integration.

To complete the step size selection, $(\omega_{PA})_{min}$ should also be determined so that the number of samples per the longest period, N_s, satisfies the accuracy requirement. This is easily computed from

$$N_s \leq 2\pi/[(\omega_{PA})_{min}\, h] \tag{41}$$

Remark: The qualifier "apparent" is used here to emphasize only those frequencies that participate in the dynamic response. Note $(\omega_{PA})_{max}$ is the highest frequency among the active frequencies that participate in the dynamic response. For example, a structure under free-fall gravity motion does not exhibit any frequency content except the rigid body motion (cf., zero frequency). In this case, $(\omega_{PA})_{max}$ is zero and the step size determined from $(\omega_{PA})_{max}$ is much larger than the critical step size based on the highest frequency of the system as determined from the eigenproblem.

8. CONCLUSIONS

In this paper the term "method" is used to include the integration formulas, the manner in which the step size changes are incorporated into the integration formulas and the step size selection strategy. We now summarize the major results of the present paper.

1. It is expedient to evaluate separately the stiffness force term and the damping term. For heavily damped problems, two evaluations of the damping term per step yield a considerable improvement on the stability margin of the central difference formula (see Table 1 for details).

2. The variable coefficient formulas are superior to the interpolated formulas for use in step change adjustments when the system is heavily damped. On the other hand, the interpolated formulas become superior when the system is lightly damped (see Table 2 for details).

3. Step size selection strategy based on the truncation error concept cannot be used for detecting the critical time step size necessary to avoid numerical instability when low accuracy is requested.

4. The proposed "perturbed apparent frequency" criteria to govern the choice of the maximum possible step size at each step has been shown to be stable when low accuracy is requested.

ACKNOWLEDGMENTS

The authors wish to acknowledge support of this work by the Office of Naval Research under Contract N00014-74-C-0355 and by the Lockheed Missiles & Space Company's Independent Research program.

REFERENCES

1 Underwood, P. G., and Park, K. C., "A Variable-Step Central Difference Method for Structural Dynamics Analysis, Part II: Implementation and Performance Evaluations", LMSC-D633782, December 1978, Lockheed Missiles and Space Company, Inc., Palo Alto, Calif.

2 Krieg, R. D., and Key, S. W., "Transient-Shell Response by Numerical Time Integration", in Advances in Computational Methods in Structural Mechanics and Design, J. T. Oden, R. W. Clough, and Y. Yamamoto, eds., The University of Alabama Press, Huntsville, Alabama, 1972, pp. 237-257.

3 Park, K. C., "Practical Aspects of Numerical Time Integration", Journal of Computers and Structures, Vol. 7, 1977, pp. 343-353.

4 Krogh, F. T., "Algorithms for Changing the Step Size by a Multistep Method, Technical Memo 275, 1971, Jet Propulsion Laboratory, California Institute of Technology, Pasadena, Calif.

5 Brayton, R. K., Gustavson, F. G., and Hachtel, G. D., "A New Efficient Algorithm for Solving Differential-Algebraic Systems Using Implicit Backward Difference Formulas, IEEE Proceedings, 60, 1972, pp. 98-108.

6 Shampine, L. F., and Gordon, M. K., Computer Solution of Ordinary Differential Equations: The Initial Value Problem, W. H. Freeman, San Francisco, Calif., 1975.

7 Zadunaisky, P. E., "On the Estimation of Errors Propagated in the Numerical Integration of Ordinary Differential Equations", Numerical Methods, Vol. 27, 1976, pp. 21-39.

8 Wilkinson, J. H., The Algebraic Eigenvalue Problem, Clarendon Press, Oxford, 1965, pp. 99-101.

9 Park, K. C., "An Efficient Implementation of Explicit Methods for Damped Second-Order Equations of Motion", Proceedings of Applications of Computer Methods in Engineering, Vol. 1, L. C. Wellford, Jr., ed., University of Southern California, Los Angeles, Calif., 1977, pp. 635-646.

10 Stetter, H. J., "Improved Absolute Stability of Predictor-Corrector Schemes", Journal of Computing, Vol. 3, 1968, pp. 286-296.

11 Gear, C. W., Numerical Initial Value Problems in Ordinary Differential Equations, Prentice-Hall, Inc., Englewood Cliffs, New Jersey, 1971.

12 Hall, G., and Watt, J. M., eds., Modern Numerical Methods for Ordinary Differential Equations, Clarendon Press, Oxford, 1976.

13 Nickell, R. E., "A Survey of Direct Integration Methods in Structural Dynamics", Technical Report No. 9, 1972, Division of Engineering, Brown University.

14 Bathe, K. J., and Wilson, E. L., "Stability and Accuracy Analysis of Direct Integration Methods", International Journal of Earthquake Engineering and Structural Dynamics, Vol. 1, 1973, pp. 283-291.

15 Park, K. C., "Evaluating Time Integration Methods for Nonlinear Dynamics Analysis", in Finite Element Analysis of Transient Nonlinear Structural Behavior, T. B. Balytschko et al., eds., ASME Applied Mechanics Symposia Series, AMD-14, 1975, pp. 35-58.

16 Gear, C. W., and Tu, K. W., "The Effect of Variable Step Mesh Size on the Stability of Multistep Methods", SIAM Journal of Numerican Analysis, Vol. 11, 1974, pp. 1025-1043.

APPENDIX A

CHARACTERISTIC POLYNOMIAL OF INTEGRATION FORMULAS FOR THE NONDIAGONALLY DAMPED CASE

Equations (8) through (11) can be expressed in matrix form as

$$\underline{A}\, \underline{y}^{n} + \underline{B}\, \underline{y}^{n-1} = 0$$

where

$$\underline{y}^{n} = \left[\ddot{u}^{n},\ \dot{u}^{n+\frac{1}{2}},\ u^{n+1}\right]$$

in which

$$\underset{\sim}{A} = \begin{bmatrix} 1 & 0 & 0 \\ h & 1 & 0 \\ 0 & h & 1 \end{bmatrix} \qquad (A.1)$$

$$\underset{\sim}{B} = \begin{bmatrix} 2\xi\omega\hat{g}, & 2\xi\omega g, & g\omega^2 \\ 0 & -1 & 0 \\ 0 & 0 & -1 \end{bmatrix}$$

$$g = 1 - \alpha\beta\,\xi\Omega$$

$$\hat{g} = (1 - \alpha)\,\gamma - \frac{\alpha}{2}(1 - \beta) - \alpha\beta\gamma\xi\Omega$$

$$\Omega = \omega h$$

The appropriate eigenproblem for (A.1a) is obtained by taking

$$\underset{\sim}{y}^{n+1} = \lambda\,\underset{\sim}{y}^{n} \qquad (A.2)$$

which is substituted into (A.1) to yield

$$(\lambda\underset{\sim}{A} - \underset{\sim}{B})\,\underset{\sim}{y} = 0 \qquad (A.3)$$

Equation (A.3) has a nontrivial solution only if

$$\det\,|\lambda\underset{\sim}{A} - \underset{\sim}{B}| = 0 \qquad (A.4)$$

Expanding (A.4), one obtains the following characteristic polynomial equation

$$\lambda(\lambda-1)^2 + g\Omega^2\lambda^2 + 2\xi\Omega g\,\lambda(\lambda-1) + 2\xi\Omega\hat{g}\,(\lambda-1)^2 = 0 \qquad (A.5)$$

Stability: In order for (8) to give a bounded solution, one must have

$$|\lambda| \le 1.0 \qquad (A.6)$$

which is the required stability condition.

Accuracy: Accuracy can be assessed by comparing the exact solution

$$\lambda_e = e^{\left(-\xi \pm j\sqrt{1-\xi^2}\right)\omega h} \qquad (A.7)$$

to the numerical solution associated with the computed damping ξ_c

$$\lambda_c = e^{\left(-\xi_c \pm j\sqrt{1-\xi_c^2}\right)\omega h} \qquad (A.8)$$

so that one can express

$$\text{frequency error (\%)} = \left(1 - \frac{\sqrt{1-\xi_c^2}}{\sqrt{1-\xi^2}}\right) \times 100 \qquad (A.9)$$

$$\text{damping error (\%)} = (1 - \xi_c/\xi) \times 100 \qquad (A.10)$$

APPENDIX B

THE EFFECT OF STEP CHANGES ON LOCAL STABILITY

The variable coefficient formula from Table 2 is

$$\dot{u}^{n+\frac{1}{2}} = \dot{u}^{n-\frac{1}{2}} + \tfrac{1}{2}(h_n + h_{n-1})\,\ddot{u}^n$$

$$u^{n+1} = u^n + h_n\,\dot{u}^{n+\frac{1}{2}} \qquad (B.1)$$

which after eliminating the velocity terms results in

$$u^{n+1} - (1 + r)\,u^n + r\,u^{n-1} = \frac{h_n^2}{2}\left(1 + \frac{1}{r}\right)\ddot{\underset{\sim}{u}}^n, \qquad r = h_n/h_{n-1} \qquad (B.2)$$

The acceleration $\ddot{u}^n$ from the basic formula can be expressed from (11a) for the modal equation (12) in the form

$$\ddot{u}^n = -g(\omega^2 u^n + 2\xi\omega\,\dot{u}^{n-\frac{1}{2}}) - 2\rho\omega\hat{g}\,\ddot{u}^{n-1}$$

where

$$g = 1 - \alpha\beta\rho\omega\,h_n/r$$

$$\hat{g} = (1 - \alpha)\,\lambda - \frac{\alpha(1-\beta)}{2} - \alpha\beta\gamma\rho\omega\,h_n/r \qquad (B.3)$$

For illustrative purposes, let us choose $\gamma = 0$, $\beta = 1$ so that combined difference equation of (B.2) and (B.3) becomes

$$u^{n+1} - (1+r)\left[1 - g\left(\frac{\Omega_n^2}{2r} + \xi\Omega_n\right)\right]u^n + \left[r - (1+r)g\,\xi\Omega_n\right]u^{n-1} = 0 \qquad (B.4)$$

Now, we use

$$u^n = \lambda_c\,u^{n-1}$$

$$u^{n+1} = \lambda\,u^n = \lambda\lambda_c\,u^{n-1} \qquad (B.5)$$

where λ_c is the amplification factor for the fixed-step case as described in Appendix A. However, the amplification factor, λ, from u^n to u^{n+1} is different from λ_c. Substituting (B.4) into (B.4), one finds

$$\lambda = (1+r)\left[1 - g\left(\frac{\Omega_n^2}{2r} + \xi\Omega_n\right)\right] - \left[r - (1+r)g\,\xi\,\Omega_n\right]/\lambda_c \qquad (B.6)$$

The effect of step changes on local stability can now be evaluated from (B.6) by requiring

$$|\lambda| \le 1.0$$

as in Appendix A, where λ_c is determined from (A.6). Other cases can be similarly evaluated via the same procedure.

A VARIABLE-STEP CENTRAL DIFFERENCE METHOD FOR STRUCTURAL DYNAMICS ANALYSIS

PART II: IMPLEMENTATION AND PERFORMANCE EVALUATION

P. G. UNDERWOOD AND K. C. PARK
Applied Mechanics Laboratory
Lockheed Palo Alto Research Laboratory
Palo Alto, California 94304

ABSTRACT

The variable-step central difference method developed in Part I is implemented as a stand-alone software package that is easily accessed by existing structural dynamics analyzers (i.e., finite-element, -difference discrete element computer codes) through a common data structure, input/output (I/O) manager and a few user-supplied control and interface routines. The performance of this package is evaluated through a computer study of four sample problems that embody a large class of response characteristics: linear to highly nonlinear; wave to structural to uncoupled component response; narrow to wide frequency spread; no damping to over-damping and accuracy-critical to numerical-stability-critical response. The present method is successful in meeting these response characteristics with effectiveness in all the above cases with the single exception of pure wave propagation.

1. INTRODUCTION

The development of a new time integration method for structural dynamics analysis not only requires a theoretically sound method but also requires an efficient implementation and evaluation procedure to determine if the method is truly viable. In this paper the implementation and evaluation procedure are presented with special emphasis on the interaction of the theoretical development with the implementation and evaluation procedure.

The variable-step central difference method described in Part I (1) is implemented as a stand-alone package as this provides the greatest possible benefit to users of the method. The modular design of the package has a minimal effect on the interior design of the host structural analyzer and changes in the time-integration method are immediately available to all users.

The performance of a computational method is very dependent on the implementation and vice versa. In this study the desired performance encompasses cost efficiency, reliability, minimum storage and I/O, and easy user interface. These performance goals are in some cases at odds with each other, hence several compromises, necessary to achieve the desired performance, were made. Fortunately, these compromises have a minimal effect on the cost efficiency and reliability.

To evaluate the performance of the implementation and the method (the two cannot be separated) four sample problems have been generated. The sample problems have a small number of degrees of freedom and may be viewed as simple, but they embody a large class of response characteristics that a successful method should be able to treat effectively. The sample problems range from linear to highly nonlinear, from wave to structural to uncoupled component response, from narrow to wide frequency spread, from no damping to overdamping and from accuracy-critical to numerical-stability-critical. With the exception of the pure wave propagation all the characteristics are effectively treated by this integration method. For one of the sample problems, a model of a drop test that has periods of free fall followed by a rebound, the variable-step method achieved a higher average step size than could be used for a stable fixed step calculation.

The paper is divided into implementation and evaluation sections. In the implementation section the functional form of the stand-alone package is discussed, followed by a presentation of the key details involved in implementing the method of Part I (1). The section concludes with a brief discussion on performance versus implementation. The numerical evaluation section presents the philosophy of the evaluation procedure followed by the results of the evaluation. In this section many of the decisions made during the development will become apparent as the effects of these decisions are easily seen.

2. IMPLEMENTATION

In this section the basic concept and implementation of a stand-alone time integration package and the specific implementation details of the variable-step central difference method presented in Part I are presented. The emphasis will be on the non-diagonal damping, the error evaluation and the step-size changing strategy techniques as these are the unique features of this method. A brief discussion of performance versus implementation concludes this section.

Stand-Alone Time Integration Package

Figure 1 presents a schematic overview of the modularized software that has evolved during the development of structural dynamic time integration procedures. This modularization has proven to be very cost effective in that existing structural dynamic analyzers are easily coupled into the time integrator software. For example, various techniques to determine the nonlinear terms are readily evaluated by interfacing with structural analyzers using different nonlinear evaluation methods. And changes in the time integrator are immediately available to all the structural dynamic analyzers, since the time integrator is a stand-alone package.

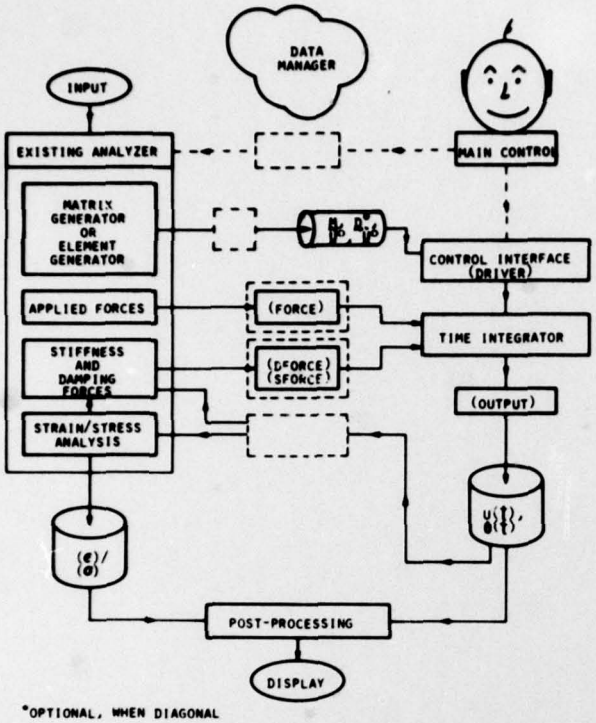

Fig. 1 Overview of structural dynamic response analysis

The term "stand-alone package" means the integrator is completely self-contained; it includes the integration method plus a local data manager that are accessed through user-supplied subroutines, indicated by parentheses in Figure 1. The dashed boxes in Figure 1 indicate that additional interfaces may be required, usually to provide a change in the data format when different local data management is used by the structural analyzer and the time integrator. To interface with the stand-alone time integrator the user must provide five subroutines (some may be dummy routines). The first (DRIVER) transmits the problem parameters, the diagonal mass matrix $\underline{M}$, (in the case of diagonal damping, $\underline{D}$ may be transmitted), and the initial conditions $\underline{u}^o$, $\dot{\underline{u}}^o$ to the time integrator. Also at the end of the time integration computations, control is returned to DRIVER. The second, an applied loads routine (FORCE), provides the load vector data to the time integrator. The third, an output routine (OUTPUT), provides display of the response. The fourth routine (DFORCE) provides the damping force as a vector; and the fifth routine (SFORCE) provides the stiffness force as a vector. Note: All data is transmitted as vectors, because diagonal matrices are treated as vectors.

The time integrator treats the governing structural dynamics equations of motion at the n-th discrete time as

$$\underline{M}\,\ddot{\underline{u}}^n + \underline{d}(\dot{\underline{u}}^n) + \underline{f}(\underline{u}^n) = \underline{P}(t^n) \qquad (1)$$

with the initial conditions $\underline{u}^o$ and $\dot{\underline{u}}^o$, where

$\underline{M}$ is the diagonal mass matrix,
$\underline{d}$ is the set of internal forces due to damping that oppose the structural velocity,
$\underline{f}$ is the set of internal forces due to stiffness that oppose the structural displacement, and
$\underline{P}$ is the applied load.

Note, in the case of linear diagonal damping, $\underline{d} = \underline{D}\,\dot{\underline{u}}^n$ ($\underline{D}$ a diagonal matrix), the elements of $\underline{D}$ (a vector) may be transmitted to the time integrator instead of supplying $\underline{d}$. The vectors $\underline{d}$, $\underline{f}$ and $\underline{P}$ are the ones transmitted to the time integrator through the user-supplied routines DFORCE, SFORCE, and FORCE. The user must assure the efficient computation of these vectors.

Time Integrator

The functional form of the stand-alone time integrator package developed during this study is illustrated in Figure 2. The package includes everything except the user-supplied subroutines which are shown to provide a reference point to Figure 1. The time integrator, inside the dashed box, is composed of the routine CENDIF/VECTOR and the associated subroutines ROTATE, ACLTN, ERROR and STEPSZ, and is controlled by the routine STINT/CENDIF. To retain simplicity the time integrator package considered in this paper is an in-core operation, but it can easily be extended to out-of-core operation for very large problems. In this section the discussion will emphasize the items in the time-loop portion of the time integrator. However, some other items will be briefly considered first.

During the opening phase, the initial values specified are those for the time integrator logic, not the initial conditions for the equations of motion. These values include arrays, counters, and switches for fixed- or variable-step integration, for printout, etc. The starting procedure means taking the first time step [i.e., correctly starting the integration; see Dahlquist (2)]. The integrator starts with a step ten times the minimum value selected by the user; this gives the integrator room to cut the step size without erroring off.

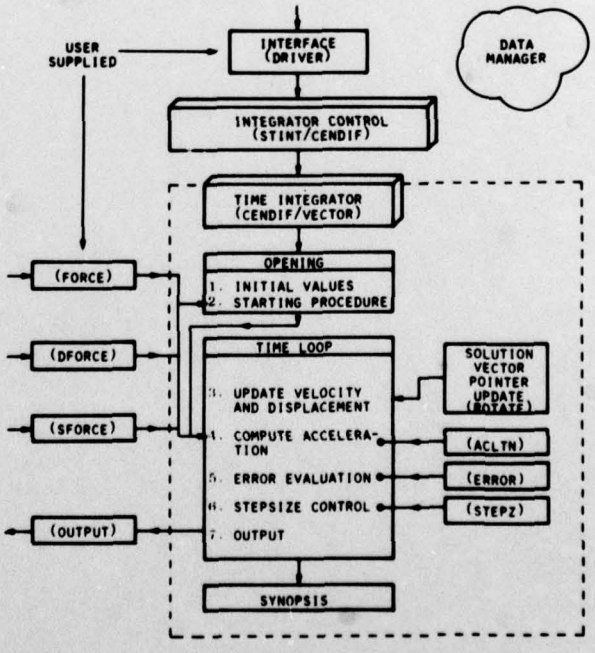

Fig. 2 Time integrator functional outline

A synopsis, summary information, is included to provide some data on the performance of the time integrator for the problem it has just solved. Printed at the end of each run, it includes the average time step, the number of step increases, the number of step decreases, the number of time steps, the number of evaluations of the equilibrium equations and a distribution count of the step sizes used during the time integration. This information is helpful in determining the efficiency of the calculations so that, as experience is gained, the user may more effectively choose input parameters for similar problems.

The time loop section of the integrator is where all the work is done. The flow of computations proceeds from Items 3 to 7 and then back to Item 3 until the problem is solved for the requested time range. Now, each item in the time loop will be discussed.

The update of the velocity and displacement for each degree of freedom depends on the conditions prevailing at that degree of freedom at the current step. After the acceleration at time t^n has been successfully computed (see below), the formulas for computing the velocity at time $t^{n+\frac{1}{2}}$ and the displacement at time t^{n+1} are chosen as shown in Table 1. The FVCO and FINT formulas were chosen for their stability characteristics under decreasing and increasing step changes; see Part I.

From Part I it is seen that to advance the step to time t^{n+1} the acceleration at time t^n must be determined. For the undamped case this is trivial; see Equation (5), Part I. For the diagonal damped case a special form is used [see equations (6) and (7), Part I] and the computation of the acceleration

Table 1 Formulas for step changes

Condition	Formula
1) $r = h_n/h_{n-1} \leq 1.0$	FVCO
2) $\ddot{u}_j^n = 0$	FVCO for component j
3) $\lvert\ddot{u}_j^n - \ddot{u}_j^{n-1}\rvert/\lvert\ddot{u}_j^n\rvert > 0.01$	FVCO for component j
4) $r > 1.0$ and conditions 2 or 3 do not apply	FINT

is not directly required. But to evaluate the error the acceleration is then determined by using equations (7) and (8) in Part I. The nondiagonally damped case is treated in Part I via equations (8) - (11). This implementation is based on $\gamma = 0$ and $\beta = 1$ and a fixed iteration cycle of predict-correct-predict. The several steps shown in Part I can be condensed. In the coding two arrays dv and w are used in conjunction with a scratch array, workb, in the following manner:

$$\underline{dv} = \underset{\sim}{M}^{-1}\,[\underline{P}^n - \underline{f}\,(\underline{u}^n)]$$

$$\underline{w} = \underline{d}\,(\dot{u}^{n-\frac{1}{2}})$$

$$\underline{w} = \dot{u}^{n-\frac{1}{2}} + \frac{\alpha}{4}\,(h_n + h_{n-1})\,(\underline{dv} - \underset{\sim}{M}^{-1}\,\underline{w}) \qquad (2)$$

$$\underline{workb} = \underline{d}(\underline{w})$$

$$\ddot{\underline{u}}^n = \underline{dv} - \underset{\sim}{M}^{-1}\,\underline{workb},$$

where α is as defined in (10), Part I, and h_n and h_{n-1} are the time step sizes for the n-th and (n-1)-th steps. In (4) the $\underline{P}^n$, $\underline{f}(\underline{u}^n)$ and $\underline{d}(\underline{x})$ terms are all obtained from the user supplied routines and the operation in the third of (2) with $\underline{w}$ on both sides of the equal sign is the standard FORTRAN replacement operation.

Now that the acceleration at the n-th step is known, the "perturbed apparent frequency" measure can be applied to determine if the solution at the n-th step is acceptable. The error is computed from equation (37) in Part I as

$$\epsilon = \max(\epsilon_1^n, \ldots, \epsilon_{MAXDEG}^n),$$

where

$$\epsilon_i^n = \frac{h_n^2}{4}\,\frac{a_i^n}{b_i^n},$$

$$a_i^n = \left|\ddot{u}_i^n - \ddot{u}_i^{n-1}\right|, \qquad (3)$$

$$b_i^n = \left|u_i^n - u_i^{n-1}\right|,$$

MAXDEG is the size of the solution vector in equation (1), and h_n is the n-th time step size. If the denominator in (3) is zero or if $|u_i^n - u_i^{n-1}|/|u_i^n| \leq 1.6 \times 10^{-8}$ for $|u_i^n| \neq 0.0$, the error is set to zero. The second condition eliminates the problem of computing an error based on machine roundoff instead of system response.

Another feature that increases the computational efficiency, but requires some knowledge of the problem at hand, is to replace the denominator term b_i^n in (3) by

$$b_i^n = \max_{|i-j|\leq m_b} (|u_j^n - u_j^{n-1}|) \qquad (4)$$

where m_b is the (average) bandwidth of the i-th degree of freedom. In the present study $m_b = 2(MAXDEG/10+1)$ has been used as an estimate when the average bandwidth was not easily determined. The above replacement for evaluating the error (3) may reduce the accuracy of some high-frequency components, but it insures that they do not grow to excess and it still produces an accurate efficient solution for the dominant response modes.

Once the error measure from (3) has been determined a decision must be made as to what step size is appropriate. The user specifies the samples per cycle (N) for the highest apparent frequency; N must be greater than π, as π is the stability limit for the central difference integrator. The number of samples per cycle converts to the error measure of (3) as

$$e = (\pi/N)^2; \qquad (5)$$

see Section 7 in Part I. Based on the ratio of the computed error (3) to the desired error (5) for the highest apparent frequency, i.e.,

$$p = \varepsilon/e, \qquad (6)$$

the step-size selection is made as shown in Table 2.

In Table 2 the condition for increase must be met for five consecutive steps to maintain reliability. The limits on the step-size change are necessary to maintain accuracy. And the restriction for S > 0.9 for step decreases is to eliminate the possibility of many small changes at one time step.

Table 2 Step size selection strategy

Conditions	Action
$0.1 \le p \le 1.0$	No change
$p < 0.1$ (for the last 5 consecutive steps)	Increase $h_{new} = S\, h_{old}$ where $S = \min [(4p)^{-\frac{1}{4}}, 1.5]$
$p > 1.0$	Decrease $h_{new} = S\, h_{old}$ where $S = (5p)^{-1/5}$ or if $S < 2/3$; $S = 2/3$ or if $S > 0.9$; $S = 0.9$

A step-size decrease indicates that the computed quantities for the n-th step do not satisfy stability or the accuracy requirements that were requested by the user, hence this step is rejected. The n-th step is again attempted by starting at Item 3 in Figure 2; this process is continued until the step size is acceptable. If the step size so determined is less than the minimum value set by the user, the code returns control to the user. If the step size is decreased more than four times at one time step, a restart of the problem is attempted at Item 2 with the last accepted displacement and velocity vectors used as initial conditions. If this fails, control returns to the user. At this point, the user must reconsider the control parameters and begin again.

If the step size is acceptable, the displacement and velocity are transmitted to the user for display purposes through the routine OUTPUT. Because the velocity is computed at half steps, extrapolated values at whole steps are provided via the formula:

$$\underline{\dot{u}}^{n} = \underline{\dot{u}}^{n-\frac{1}{2}} + \tfrac{1}{2} h_n \underline{\ddot{u}}^{n}, \qquad (7)$$

where h_n is the n-th step size.

It should be emphasized that many of the decisions involved in this implementation are based on numerical experiments with a limited class of problems. Hence, for another set of problems, one might utilize a different set of decisions. The subjective decisions are: 1) the coupling concept to determine the denominator in equation (3); 2) the limits on p, especially the lower one; and 3) the factors 1.5, 2/3 and 0.9 that appear in Table 2.

The coding required for the variable-step central difference time integrator is obviously more involved than that for a simple fixed step version. But the cost differences in computing with a fixed step versus variable steps are minimal, especially when one considers the power of the variable step method. In some cases the variable-step method has been found to be cheaper than the fixed-step method even if the maximum fixed-step size could be accurately determined a priori.

Performance versus Implementation

The performance of a time integration software package can be considered from two perspectives: 1) the overall performance of the complete package; and 2) the performance of the time integrator. The first addresses the ease of use, I/O requirements and overall efficiency, whereas the second is related to the computational efficiency of the method. If the performance is poor in either area, the usefulness of the package is weakened.

In the authors' programming environment the stand-alone package implementation has greatly increased performance. Usually, new problems require the adaptation of existing software to produce some new analysis capability. With an existing operational time integration package and using a common I/O manager for all software, a transient response analysis package can be built very quickly by very simply plugging modules together. Of course, in a strictly production analysis environment, a time integrator embedded in the coding may be more desirable; see Felippa and Park (3) for further discussion of this subject.

For the time integrator the performance is a strong function of the reliability of the method. A totally reliable variable-step time integrator would be costly, but in a majority of cases near total reliability with modest costs can be obtained. For this implementation a large number of samples per cycle, approximately 4π, plus error evaluation based on each degree of freedom will produce close to total reliability. The most efficient (time and cost of computer operation) is obtained with a sampling of π and error evaluation based on coupled degrees of freedom. Experience has shown that this later approach is roughly 80% reliable, i.e., the integration remains stable and produces a reasonably accurate solution (10% error at most).

In the coding of the method, the biggest compromise was made in core storage used for the computations. To keep the cost down, it was found that using scratch arrays to cut down on the number of DO-loops, and saving the three most current displacements, velocity and acceleration vectors to enable backtracking without restarting and for error evaluation was required. This limits the problem size that can be solved in-core to between 700 and 1800 degrees of freedom depending on the damping option and time step option. This is still a fairly respectably-sized problem for dynamic analysis, so it is not considered limiting.

3. EVALUATION

The development of a new integration method and its computer implementation must be complimented by a series of evaluation tests to assess its effectiveness in engineering analysis environments. Four simple structural dynamic models have been chosen that cover a wide range of dynamic characteristics that are useful in evaluating various algorithms and implementations. In this section the performance of the variable-step central difference method will be illustrated using these models.

The four models are a four-wheel dolly, a drop test, a cantilever beam, and an axial bar; these

are described in detail in Appendix A. The four-wheel dolly model has a relatively narrow band of frequency components, roughly 20% damping and the response is characterized by an initial transient, followed by a damped free vibration. The drop test model also has a narrow band of frequency components, 10% and 110% damping elements and the response is the highly nonlinear motion of a package falling to the ground, impacting the ground, rebounding, falling, impacting, etc. The cantilever beam is a simple beam bending model including translational and rotational degrees of freedom, hence a fairly stiff (wide frequency range) problem. Both linear and nonlinear bending characteristics are considered for the undamped response to a tip step load. The axial bar is a simple model of wave propagation in a free-free bar subjected to an initial displacement. These models cover a wide range of characteristics encountered in a structural dynamic analysis: linear to highly nonlinear; wave to structural to uncoupled component response; narrow to wide frequency spread; no damping to overdamping; and accuracy-critical to numerical-stability-critical response.

Four-Wheel Dolly (Moderate Damping, Narrow Frequency Spread)

The computed displacements of wheels 1 and 4 and the force between ground and wheels 1 and 4 for the four-wheel dolly are shown in Figure 3. Note the displacements exhibit early time high frequency and late time low frequency. The spring force at wheel 1, FK_5, shows that wheel 1 lifted off the ground between 0.02 and 0.04 seconds and again for an instant just after 0.1 seconds and the spring force at wheel 4, FK_8, shows that wheel 4 lifted off the ground between 0.07 and 0.09 seconds.

The time step size histories for different accuracy specifications are shown in Figure 4. The highest average time step was obtained with a sampling of π samples/cycle of the highest apparent frequency; this is the minimum sampling to obtain numerical stability. The lowest average time step was obtained with a sampling of 3π samples/cycle of the highest apparent frequency; this provides a very accurate solution. Both computations were made with $\alpha = 1.0$; see (2) and the discussion below. The middle average time step size shown in Figure 4 was obtained from a truncation error control method; see Part I (1). Note that both 3π sampling apparent frequency and truncation error methods used a relatively small step size and actually reduced the step size some during the initial transient nonlinear response. This indicates that accuracy is controlling the integration during this phase. The 3π sampling computations show that after the initial transient the step size variation settles down but does not increase very much as the requested accuracy is controlling the step size. The π sampling computations illustrate that the step size generally increases throughout. The step size is increased very rapidly and maintains a large step size resulting in a very quick computation that is still quite accurate (within 5% of the most accurate computation made for this problem). These curves, Figure 4, show the effectiveness of the perturbed apparent frequent measure. On the other hand, for a low-accuracy but stable run with the truncation error concept, the best obtainable is the one shown in Figure 4. If a lower accuracy were requested it would increase the step size quickly but would go unstable at later times; if a higher accuracy were requested the average step size would be painfully small. Also, the truncation error method does not produce the consistency that is shown by the apparent frequency method.

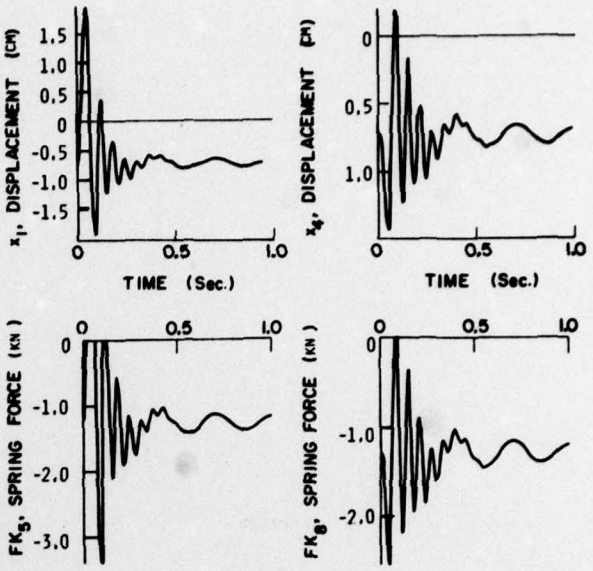

Fig. 3 Four-wheel-dolly response

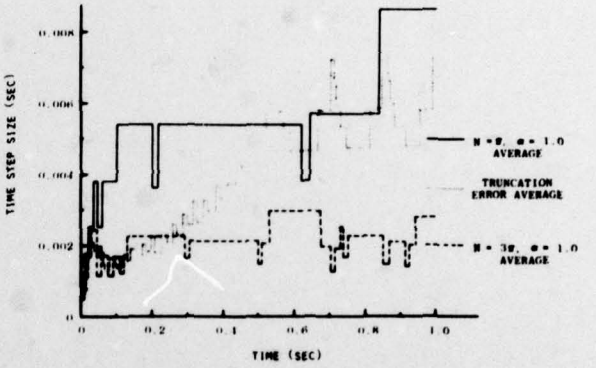

Fig. 4 Four-wheel-dolly step size histories

In Part I the influence of the parameter α on stability and accuracy was analyzed; this influence is verified in Table 3, which summarizes some results for the four-wheel-dolly response. The effect of various values of α on the average step size, computer time, and the accuracy of the maximum displacement of wheel 1 and the minimum acceleration of wheel 2 (chosen as they are the most sensitive) is considered. For both sampling rates (π and 3π) the average step size and hence the computer time is essentially the same indicating that α does not influence the stability limit for a moderately damped (approximately 20%) problem; this is in agreement with Figure 1 of Part I. On the other hand, the accuracy is influenced by the choice of α; the values given for displacement and acceleration for $N = 3\pi$, $\alpha = 1.0$ are the most accurate and compare very well with other known accurate integration methods. Notice that in all cases the accuracy improves as α increases; this is in agreement with Figures 2a and 2c of Part I. This problem was also run for two fixed step cases corresponding to the average time step for the $N = \pi$ and 3π, $\alpha = 1.0$ cases. It is seen that the fixed step computations are essen-

Table 3 Four-wheel-dolly summary

Sample	α	$\Delta t_{average}$ (sec)	CAU (sec)	TOTAL (sec)	$X_{1_{max}}$ (cm)	$\ddot{X}_{2_{min}}$ (m/sec^2)
π	0.4	0.0049261	3.333	15.996	1.83723	-2.55092
π	0.5	0.0049261	3.332	15.950	1.83919	-2.43147
π	0.6	0.0046948	3.489	16.109	1.85042	-2.30810
π	0.8	0.0049261	3.340	15.952	1.85704	-2.13868
π	1.0	0.0048780	3.365	15.952	1.86410	-1.89901
3π	0.4	0.0020619	6.280	19.981	1.85539	-2.27239
3π	0.5	0.0020661	6.280	19.947	1.85758	-2.17632
3π	0.6	0.0022026	5.950	19.484	1.85953	-2.13606
3π	0.8	0.0021505	6.084	19.673	1.86365	-2.05329
3π	1.0	0.0020661	6.270	19.865	1.86807	-1.99542
Fixed Step	1.0	0.0048780	3.575	16.538	1.93251	-1.91671
Fixed Step	1.0	0.0020661	6.788	21.192	1.87259	-1.98775

tially equivalent in computer time to the variable step computations; hence there is minimal overhead involved in using the variable step feature. Secondly, note that the accuracy for the larger step size run is poorer than for the comparable variable step run. This occurs because the variable step run used a smaller initial time step when the response is accuracy critical. There appears to be little reason to recommend a fixed step computation.

Drop Test (Heavily Damped, Component Responses)

Two representative response histories for the drop test problem are shown in Figure 5; the displacement of degree of freedom 7, the base, and the acceleration of degree of freedom 5, the 10% damped-100 Hz oscillator. When the displacement is less than 0.0 the base is in contact with the nonlinear spring representing the ground, the positive slope portions of the displacement response indicate rebound and the negative slope portions indicate free fall conditions for displacements greater than 0.0. The response is like a bouncing ball. Whenever the structure contacts the ground a shock is felt by the oscillators, indicated by the sharp spikes seen on the acceleration response. These spikes dampen out and during the free fall a constant free fall acceleration of -9.8 m/s^2 is obtained.

The step size history for a calculation with 3π samples/cycle of the highest apparent frequency and α = 0.25 is shown in Figure 6. During the initial free fall the step size increases very rapidly, since the apparent frequency of this initial free fall is zero. Once the initial impact occurs the step size is decreased and after this the step size never returns to its early high value since the oscillations of the various components restrict the maximum step. It is generally seen that the step size is decreased upon impact and increases during free fall, although the general pattern is somewhat clouded by the very difficult accuracy and stability conditions presented by the overdamped degrees of freedom.

This problem can be successfully run for a fixed time step of 0.001 sec, but for 0.0015 sec the calculations become unstable. From Figure 6 it is seen that the minimum step size is slightly less than 0.001 sec and this appears to be dictated by stability considerations based on the fixed-step calculations. Here the variable-step method is clearly superior to the fixed-step method. The variable-step method takes advantage of the instantaneous conditions to run with a near

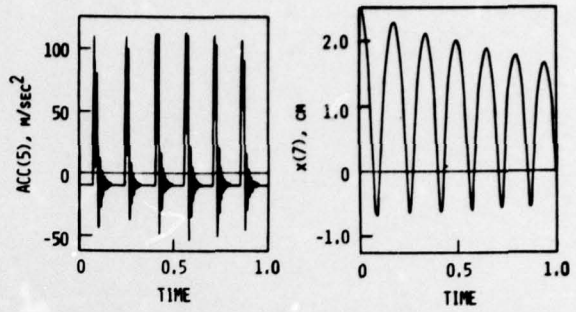

Fig. 5 Drop test response

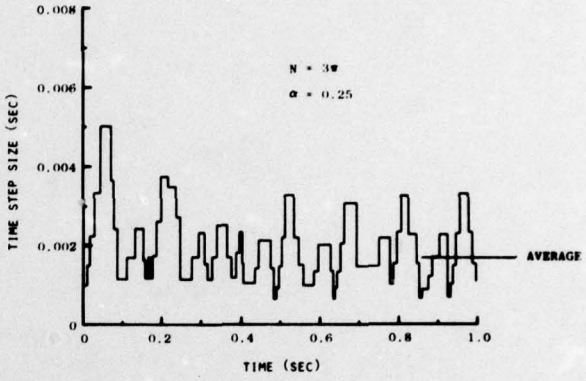

Fig. 6 Drop test step size history

optimum step size while the fixed step size must be restrictively small to maintain stability during critical portions of the response.

In the preceding section, "Time Integrator", the use of the FINT formula for increasing step sizes under constant or near-constant acceleration was presented. The need for this computational detail was made apparent during the evaluation studies of the drop test problem. During the initial free fall under constant gravity acceleration, the calculations exhibited a mild instability which contaminated the subsequent calculations and error control when the FVCO formula was used to compute the response. By switching to the FINT formula to take advantage of the more uniform stability limit for all damping ratios (see Figure 3 of Part I) this problem area was eliminated.

The behavior of the drop test model response is summarized in Table 4 for various samplings and α's. For a fixed α (α = 0.25) the average step size decreases for increased sampling rate in a very consistent manner. For the 2π sampling rate, variations in α cause large variations in the maximum computed acceleration. For the lower values of α the maximum acceleration occurs at degree of freedom 5, the high-frequency lightly-damped oscillator. But for the higher values of α the maximum acceleration occurs at degree of freedom 6, the high-frequency overdamped oscillator. This indicates that for heavily damped problems a fairly small α should be used to preserve accuracy. This result is foreseen in Part I, but from the numerical experiments it is seen that an α samller than that considered in Part I should be used. The acceleration results show that for a low sampling rate or a larger α the overdamped response is the most difficult to control from both stability and accuracy viewpoints.

Table 4 Drop test summary

Sample	α	$\Delta t_{average}$ (sec)	CAU (sec)	TOTAL (sec)	$\lvert x \rvert_{max}$ (cm)	$\lvert \ddot{x} \rvert_{max}$ (m/sec^2)
π	0.25	0.0018553	5.741	18.887	43.208^{*}_{1}	1092.911^{*}_{6}
3π/2	0.25	0.0017889	5.912	19.034	43.172_{1}	379.679_{5}
2π	0.25	0.0017452	6.074	19.313	43.071_{1}	164.338_{5}
2π	0.30	0.0019194	5.587	18.778	43.007_{1}	139.682_{5}
2π	0.40	0.0024096	4.592	17.337	42.934_{1}	279.375_{6}
2π	0.50	0.0023041	4.772	17.553	42.890_{1}	1023.493_{6}
3π	0.25	0.0017094	6.189	16.913	42.959_{1}	123.500_{5}
4π	0.25	0.0016779	6.197	19.478	42.934_{1}	116.035_{5}

* Subscripts indicate degree of freedom

The displacement results show that for a low-frequency, lightly-damped element very good accuracy is obtained for any combination of sampling and α. The major conclusion is that for heavily damped problems an $\alpha = 0.25 \rightarrow 0.30$ should be used and a sampling rate of at least 2π should be used to maintain accuracy and stability. This is especially true when the highest frequency component is also one of the heavily damped components as in this example.

Cantilever Beam (Wide Frequency Spread)

The tip rotation and displacement (degrees of freedom 1 and 2) for the linear cantilever beam response is illustrated in Figure 7 for variable-step computations based on the apparent frequency and the truncation error step control methods. For all sampling rates of π or greater, the response computations based on the apparent frequency method are essentially identical for displacements; only the accelerations exhibit a converging pattern for increasing sampling rates. This is due to the widely spread frequency content of this problem in which the overall displacement response is composed of low-frequency components while the high-frequency components are controlling the step size. Figure 7 shows the truncation error control rotational response has a very high frequency hash of relatively large magnitude superimposed on the actual response. This hash appears because the truncation error control was unable to detect the stability limit until the step size exceeded the stable step size. It was found that for any specified error of reasonable magnitude the truncation error control method was unable to maintain a stable integration for the cantilever beam. For extremely low error (high accuracy) the truncation error control remains stable but the average step size is at least an order of magnitude less than the stable step size. On the other hand, for the π sampling rate the apparent frequency method achieves an average step size that is roughly 85% of the stability limit. Also this method is able to increase the time step very rapidly up to the maximum step size used and maintain this step size for the majority of the computations. Hence, the average step size is nearly equal to the maximum step size.

The results for various sample rates for the linear and nonlinear cantilever beam response are summarized in Table 5. Notice that as the sampling rate increases the average step size decreases in a consistent manner. The displacement is converged for all

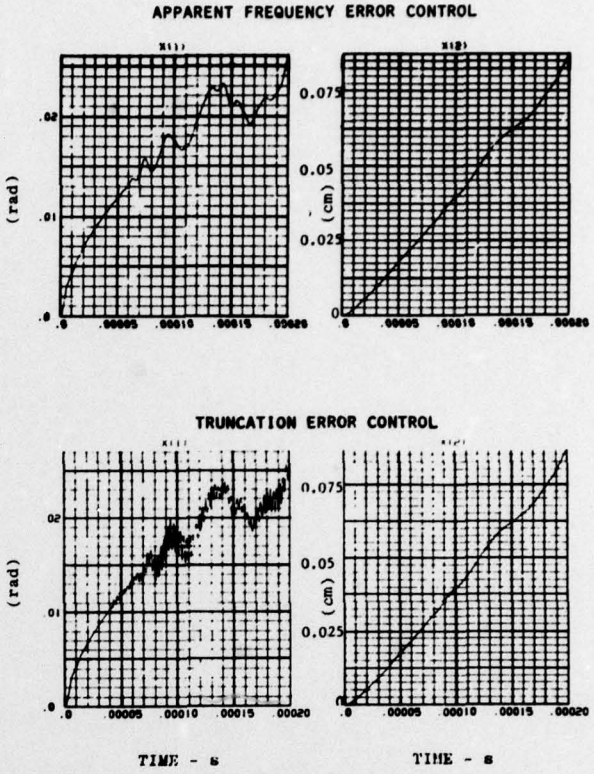

Fig. 7 Cantilever beam tip rotation and displacement response

Table 5 Cantilever beam summary

Sample	$\Delta t_{average}$ (μsec)	CAU (sec)	TOTAL (sec)	$\lvert x_2 \rvert_{max}$ (cm)	$\lvert \ddot{x}_1 \rvert_{min}$ (km/sec^2)
		Linear Cantilever Beam			
π	0.66445	7.802	21.266	0.08878	6676.64
3π/2	0.47962	10.176	24.093	0.08877	7998.71
2π	0.33113	13.775	28.410	0.08877	7131.56
3π	0.29445	15.196	30.162	0.08877	7224.52
4π	0.18657	22.840	39.794	0.08877	6694.93
		Nonlinear Cantilever Beam			
π	0.61728	9.349	23.214	0.11575	7503.16
3π/2	0.51414	10.664	24.827	0.11575	5304.03
2π	0.36496	13.941	28.768	0.11573	5688.08

sampling rates and the acceleration shows some randomness but the deviation is very small especially if the comparison is made among the higher sampling rates. The nonlinear response shows that softening of the bending properties of the beam generally increases the average step size as would be expected. The only discrepancy in these observations is seen at the π sam-

pling; this is probably due to slight steps over the stability boundary. The parameter α has no influence on the undamped problem, so it is not considered.

Axial Bar (Wave Propagation)

The exact solution for an initial displacement of 2.54 cm at the center node of the bar (actually a triangular spatial displacement of 0.0 at the nodes on either side of the center and 2.54 cm at the center) is two triangular displacement pulses of half the original magnitude, one traveling in the negative direction and the other in the positive direction. At the free boundary this pulse is reflected. If this model is run with the time step equal to the critical time step (fixed-step computation) the numerical results are exact, as shown in the left half of Figure 8 for the displacement response at nodes 11, 14, and 17. Note the magnitudes and arrival times are exact. The variable-step method, presented in this paper, produces the correct results if one starts with the critical time step and uses a sample rate of π; i.e., the time step is never increased or decreased. Hence, the apparent frequency concept functions properly for the wave propagation problem. But at any other initial time step the error computation detects an error and then the step size is always decreased. The response is the hashy junk shown in the right-hand half of Figure 8. The problem of the proper error control for a pure wave propagation response has not been resolved. This will have to consider the shape of the error-step size curve so that the slope of the curve can enter into the decision whether to increase or decrease the step size to reduce the error.

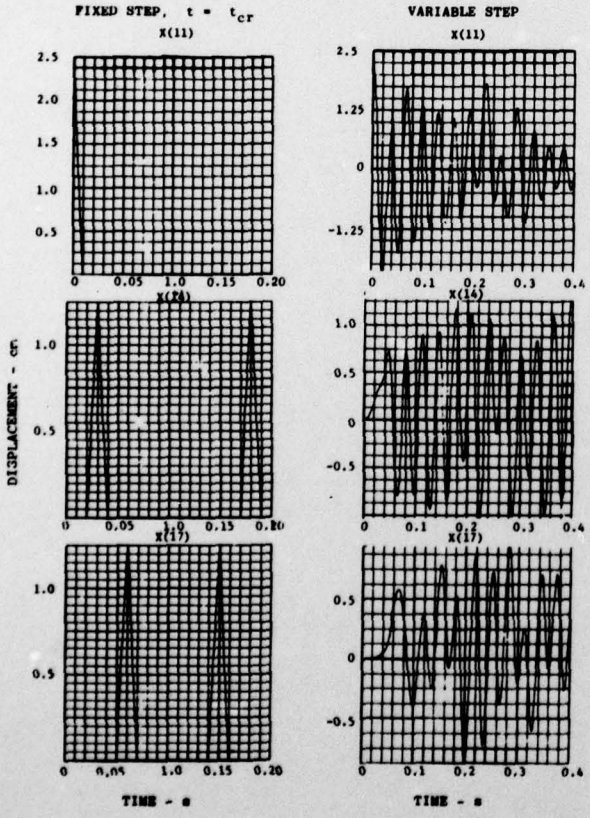

Fig. 8 Axial bar response

4. CONCLUSIONS

The implementation of the variable-step central difference method developed in Part I as a stand-alone software package has been shown to be a viable product. The package is cost efficient and easily accessed by existing structural analyzers. The evaluation of the method showed that the apparent frequency concept is vastly superior to the truncation error for controlling stability and accuracy. Of the wide range of problem characteristics considered only pure wave propagation is not properly controlled by the step size selection strategy presented here. The wave propagation control problem is being investigated and the resolution of the problem will be reported in a future publication.

ACKNOWLEDGMENT

The authors wish to acknowledge support of this work by the Office of Naval Research under Contract N00014-74-C-0355 and by the Lockheed Missiles & Space Company's Independent Research program.

REFERENCES

1 Park, K. C., and Underwood, P. G., "A Variable-Step Central Difference Method for Structural Dynamic Analysis, Part I - Theoretical Aspects", LMSC-D626886, July 1978, Lockheed Palo Alto Research Laboratory, Palo Alto, California.

2 Dahlquist, G., and Björk, A., Numerical Methods, Prentice-Hall, Inc., Englewood Cliffs, New Jersey, 1974.

3 Felippa, C. A., and Park, K. C., "Direct Time Integration Methods in Nonlinear Structural Dynamics", presented at the International Conference on Finite Elements in Nonlinear Mechanics (FENOMECH 1978), ISD, Universität Stuttgart, Stuttgart, West Germany, 30 August - 1 September 1978.

APPENDIX A

EVALUATION MODELS

The discrete models used to evaluate the time integrator are presented in this appendix. A brief physical description and a sketch of each model is given. The numerical values of the masses, dampers, springs, loads and initial conditions are presented so that the problem can be modeled by the interested reader.

FOUR-WHEEL DOLLY

The first model is a four-wheel dolly that has a short transient period followed by damped free vibration. The model is shown in Figure A-1 and the properties data are given in Table A-1. Masses 1-4 represent the four wheels, mass 5 the translation inertia and masses 6 and 7 the rotation inertias of the dolly. Springs and dampers 1-4 represent a linear suspension system and springs 5-8 represent the nonlinear spring characteristics of a wheel in contact with the ground, i.e., linear in compression and zero force in tension. A constant force of -5151.04N (-1158 lbs) is applied to mass 5 to represent the dead load; along with initial displacements of $x_1 = x_2 = x_3 = x_4 = -0.007353$m (-0.2895 in.) and $x_5 = -0.022060$m (-0.8685 in.) to place the dolly in equilibrium. The excitation is provided by an isosceles triangle pulse of 2224.11N (500 lbs) peak at 0.025s applied to mass 1, representing a severe bump encountered by wheel 1. This tran-

sient load is severe enough to first lift wheel 1 off the ground and then wheel 4 on the rebound. So the motion of the dolly is a rotation about the axis formed by wheels 2 and 3 along with some translation. After the transient and nonlinear rebound phase the dolly rocks back and forth with the motion dampening out. Hence during this problem there is a transient phase of higher frequency response followed by a long free vibration phase of lower frequency.

DROP TEST

The second model is a drop test package that is dropped onto a nonlinear spring, representing the ground. The model is shown in Figure A-2 and the properties data are given in Table A-2. Mass 7 is seen to represent a large rigid portion of a structure with internal packages (components) represented by masses 1-6, and dampers and springs 2-7. Spring 1, tabulated in Table A-2, is a nonlinear spring giving an approximate system frequency of 10 Hz that represents the ground or some surface upon which the package is dropped. The first two oscillators, m_1 and m_2, are 1.0 Hz oscillators (undamped) and with the first oscillator damped at 10% of critical and the second at 110% of critical. The next pair of oscillators, m_3 and m_4, are 10 Hz oscillators with the same damping characteristics and the last pair of oscillators, m_5 and m_6, are 100 Hz oscillators with the same damping characteristics. The initial displacement of all the masses (degrees of freedom) is 0.0254m (1.0 in.). A force of -1717.01N (-386.0 lbs) is applied to masses 1-6 and a force of -171701.37N (-38600.0 lbs) is applied to mass 7; this represents the gravitational force. With these conditions the response is composed of periods of free fall, a shock excitation, rebound, free fall, etc.

CANTILEVER BEAM

The third model is a cantilever beam with both linear and nonlinear stiffness characteristics subjected to a lateral tip load (step time function). The model is shown in Figure A-3 and the properties data are given in Table A-3. The cantilever beam is discretized with 14 equal mass elements with rotational and translational degrees of freedom. The stiffness is characterized by bending and shear springs; no damping is considered. The discrete elements are based on the properties for a continuum beam with the dimensions and properties as shown in Figure A-3. The nonlinear model considers nonlinear bending stiffness only; the shear stiffness remains linear. The connection to physical reality is tenuous, but it can be thought of as a two-strip cantilever beam of the same total thickness that has been riveted together. The moment-rotation relationship remains linear for a small rotation and then is nonlinear, indicating some slipping of the riveted joints. The purpose of the nonlinear model is to compare the behavior of the time step selection logic to that for the linear model and to determine the computational overhead for a nonlinear model. The excitation is a step (at zero time) load of 889.64N (200 lbs) applied at degree-of-freedom 2 in the positive direction.

AXIAL BAR

The fourth model is an axial bar subjected to wave propagation. The model and properties are given in Figure A-4. Note the properties are chosen to give a maximum frequency of 200 rad/sec, hence a maximum time step of 0.01 sec for the central difference method. The initial condition is a displacement of 0.0254m (1.0 in.) at degree-of-freedom 11, i.e., at the center of the bar.

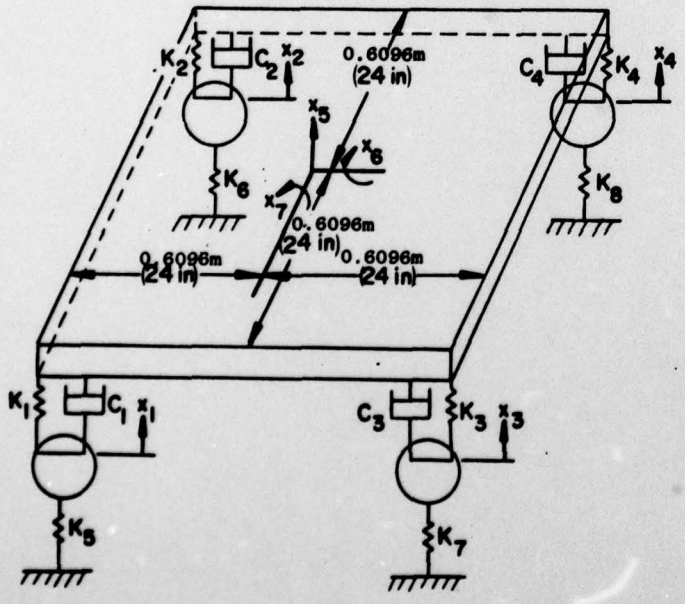

Fig. A-1 Four-wheel-dolly model

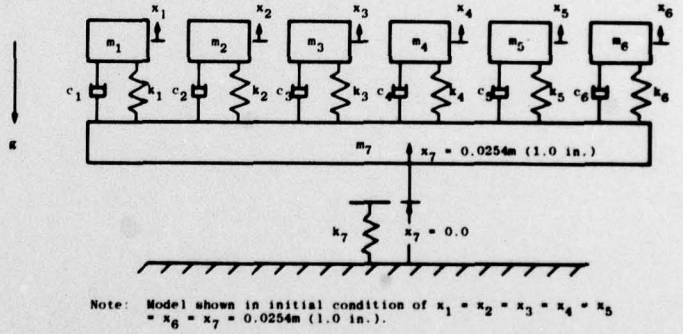

Fig. A-2 Drop test model

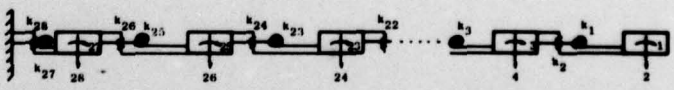

Fixed-Free Cantilever Beam

Length	0.1778 m	(7.0 in)
Thickness	0.00508 m	(0.20 in)
Weight/Density	17915.5 N/m^3	(0.066 lb/in^3)
Elastic Modulus	2.89x10^{11} N/m^2	(42x10^6 lb/in^2)

Model

- 14 equal mass elements of 0.0127 m (0.5 in) length
- Translational and rotational inertia
- Shear and bending springs
- Undamped

Fig. A-3 Cantilever beam model

Table A-1 Structural dynamic properties of the four-wheel-dolly model

Number	Mass		Dampers		Springs	
	(kg)	((lb-sec^2/in))	(N·S/m)	((lb-sec^2/in))	(M/m)	((lb/in))
1	8.7563	(0.05)	700.51	(4.0)	87563.43	(500.0)
2	8.7563	(0.05)	700.51	(4.0)	87563.43	(500.0)
3	8.7563	(0.05)	700.51	(4.0)	87563.43	(500.0)
4	8.7563	(0.05)	700.51	(4.0)	87563.43	(500.0)
5	525.3804	(3.00)			175126.85	(1000.0)*
6	10507.6080	(60.00)			175126.85	(1000.0)*
7	10507.6080	(60.00)			175126.85	(1000.0)*
8					175126.85	(1000.0)*

* Compression only, no spring in tension

Table A-2 Structural dynamic properties of the drop test model

Number	Mass		Dampers		Springs	
	(kg)	((lb-sec^2/in))	(N·S/m)	((lb-sec/in))	(N/m)	((lb/in))
1	175.1268	(1.0)	220.07	(1.25664)	6913.73	(39.4784)
2	175.1268	(1.0)	2420.78	(13.8230)	6913.73	(39.4784)
3	175.1268	(1.0)	2200.71	(12.5664)	691372.79	(3947.84)
4	175.1268	(1.0)	24207.78	(138.230)	691372.79	(3947.84)
5	175.1268	(1.0)	22007.14	(125.664)	69137278.51	(394784.0)
6	175.1268	(1.0)	242077.85	(1382.30)	69137278.51	(394784.0)
7	17512.68	(100.0)	0.0	(0.0)	*	*

* Force-Deflection Characteristics of Spring 7

Deflection		Force	
m	(in)	N	(lb)
-2.54	(-100.0)	-556027.75	(-125000.0)
-0.007620	(-0.3)	-556027.75	(-125000.0)
-0.005080	(-0.2)	-1779288.80	(-400000.0)
-0.002540	(-0.1)	-444822.20	(-100000.0)
-1.27x10^{-7}	(-0.000005)	-4448.22	(-1000.0)
0.0	(0.0)	0.0	(0.0)
2.54	(100.0)	0.0	(0.0)

Table A-3 Structural dynamic properties of the cantilever beam model

Number	Mass		Spring	
1-25 (odd)	4.022×10^{6} kg·m^2	(3.56×10^{-5} in-lb·sec^2/rad)	6327.15 m·N	(5.6×10^{4} in-lb)*
2-26 (even)	0.29947 kg	(1.71×10^{-3} lb·sec^2/in)	1.1208×10^{9} N/m	(6.4×10^{6} lb/in)
27	4.022×10^{-6} kg·m^2	(3.56×10^{-5} in-lb·sec^2/rad)	12654.30 m·N	(1.12×10^{5} in-lb)*
28	0.29947 kg	(1.71×10^{-3} lb·sec^2/in)	2.2416×10^{9} N/m	(1.28×10^{7} lb/in)

* For nonlinear model the following tabular values are used:

θ (rad)	Moment** (m·N)	Moment** (in·lb)
-1.00	-3164.21	(-2.80056×10^{4})
-0.002	-6.9599	(-61.6)
-0.001	-6.3272	(-56.0)
0.0	0.0	(0.0)
0.001	6.3272	(56.0)
0.002	6.9599	(61.6)
1.00	3164.21	(2.80056×10^{4})

** For spring 27 multiply by 2.0

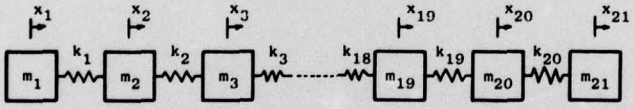

m_{1-21} = 175.12685 kg (1.0 lb·sec^2/in)

k_{1-20} = 1751268.5 N/m (10000.0 lb/in)

Boundary Conditions: Free-Free

Fig. A-4 Axial bar model